CONVERGENT FINITE ELEMENT APPROXIMATIONS OF SURFACE EVOLUTION WITH RELAXED MINIMAL DEFORMATION

GUANGWEI GAO[†], BUYANG LI[†], AND RONG TANG[*†]

Abstract. The finite element approximation of surface evolution under an external velocity field is studied. An artificial tangential motion is designed by using harmonic map heat flow from the initial surface onto the evolving surface. This makes the evolving surface have minimal deformation (up to certain relaxation) from the initial surface and therefore improves the mesh quality upon discretization. By exploiting and utilizing an intrinsic cancellation structure in this formulation and the role played by the relaxation term, convergence of the proposed method in approximating surface evolution in the three-dimensional space is proved for finite elements of degree $k \geq 4$. One advantage of the proposed method is that it allows us to prove convergence of numerical approximations by using the normal vector of the computed surface in the numerical scheme, instead of evolution equations of normal vector (as in the literature). Another advantage of the proposed method is that it leads to better mesh quality in some typical examples, and therefore prevents mesh distortion and breakdown of computation. Numerical examples are presented to illustrate the convergence of the proposed method and its advantages in improving the mesh quality of the computed surfaces.

Keywords: Surface evolution, evolving FEM, mesh quality, tangential motion, convergence.

1. Introduction

We consider the evolution of a two-dimensional surface $\Gamma(t)$ under a prescribed velocity field u in the three-dimensional space. The evolving surface $\Gamma(t)$ can be represented as the image of the flow map $X(\cdot,t) : \Gamma^0 \to \mathbb{R}^3$, satisfying

$$\partial_t X(\cdot,t) = u(X(\cdot,t),t) \quad \text{on } \Gamma^0, \tag{1.1}$$

with the initial condition $X(\cdot,0) = \mathrm{id}$ on Γ^0, where id denotes the identity map such that $\mathrm{id}(x) = x$ for $x \in \mathbb{R}^3$. The development of numerical approximations for surface evolution described by (1.1) is fundamental for solving partial differential equations (PDEs) on dynamically evolving surfaces [27, 28, 35, 16, 36, 21, 19, 22, 20, 23], as well as PDEs in bulk domains with moving boundaries or interfaces. The evolution of surfaces or interfaces can also be integrated with fluid dynamics such as two-phase fluid flow [29, 3, 12, 30] and fluid-structure interaction [42]. Additionally, the numerical techniques for solving (1.1) are intimately connected to the approximation of geometric flows [13, 4, 14, 15, 25, 38], underscoring their broad applicability and significance in computational mathematics and applied sciences.

However, approximating surface evolution through numerical methods presents significant challenges, particularly in maintaining the quality of the surface mesh. A key difficulty lies in the potential of mesh distortion and degeneration over time, with nodes possibly clustering and mesh distorting, especially when an evolving surface undergoes large deformation. Such issues can result in breakdown of computation or substantial errors in approximating the shape of an evolving surface. Furthermore, when surface evolution is coupled with PDEs in the bulk domain enclosed by the surface, the quality of the approximate surface mesh directly affects the accuracy of the numerical solutions to these PDEs. To address these challenges, re-meshing techniques have been developed [4, 39, 41, 43]. These techniques can be employed to restore mesh quality when it falls below a certain threshold, thereby ensuring reliable and accurate numerical approximations of surface evolution and the associated PDEs.

2010 *Mathematics Subject Classification.* 65N30, 65R20.

[†]Department of Applied Mathematics, The Hong Kong Polytechnic University, Hong Kong. Email address: guang-wei.gao@polyu.edu.hk, buyang.li@polyu.edu.hk, claire.tang@polyu.edu.hk.

[*]Corresponding author.

An alternative approach to re-meshing is the introduction of artificial tangential motion of the evolving surface, which does not alter the shape of the evolving surface but improves the mesh quality of the approximate surface. In their seminal works [10, 8, 9], Barrett, Garcke, and Nürnberg (BGN) introduced a class of weak formulations that use the same normal velocity as the geometric flow while incorporating artificial tangential motion which makes the map from surface Γ_h^j to surface Γ_h^{j+1} approximately harmonic (since harmonic map between surfaces tends to keep the shape of triangles unchanged), where Γ_h^j denotes the approximate surface at the time level $t = t_j$. Their method, known as the BGN method for this specific choice of artificial tangential motion, has been extensively adopted and extended in the development of numerical methods for various applications, including the development of energy-stable and volume-preserving finite element methods (FEMs) for surface diffusion [5], interface evolution in two-phase Navier-Stokes flow [12, 29, 30], solid-state dewetting with contact line migration [6, 44, 7], and elastic flow with junctions [11].

The rigorous proof of convergence of the BGN methods for various problems remains open. The convergence of a stabilized version of the BGN method for one-dimensional curve evolution under curve shortening flow was proved in [2] recently. However, the error analysis for the stabilized BGN method still cannot be extended to general two-dimensional surfaces with triangular mesh due to its necessity of using one-dimensional mass-lumping techniques.

In addition to the BGN methods, an alternative approach for constructing artificial tangential velocity to improve mesh quality of approximate surfaces was proposed by Elliott & Fritz in [37, 26]. In this method, the tangential velocity is generated by a reparametrization of the surface using DeTurck flow techniques. This approach enables the proof of convergence for evolving FEMs that incorporate tangential motion. Convergence of evolving FEMs has been successfully shown for curve shortening flow [37] and mean curvature flow of closed torus-type surfaces [40]. However, proving the convergence of this class of algorithms for general surfaces in three dimensions remains an open and challenging problem.

In [31], Hu & Li showed that, as the time stepsize tends to zero, the velocity produced by the temporally semidiscrete BGN method (without spatial discretization) formally converges to a limit velocity v satisfying the following equations:

$$\begin{aligned} v \cdot n &= u \cdot n \qquad \text{on } \Gamma(t) \\ \Delta_{\Gamma(t)} v &= \kappa n \qquad \text{on } \Gamma(t), \end{aligned} \tag{1.2}$$

where u is the original velocity of the surface, n is the unit ourward normal vector of surface $\Gamma(t)$, and κ is an unknown scalar function on $\Gamma(t)$. It is shown that the tangential velocity determined by equation (1.2) minimizes the following energy under constraint $v \cdot n = u \cdot n$:

$$E_{\mathrm{DR}}[X(\cdot, t)] = \frac{1}{2} \int_{\Gamma(t)} |\nabla_{\Gamma(t)} v|^2,$$

which represents the deformation rate of the surface, and the function κ in (1.2) represents a Lagrange multiplier arising from the constrained optimization problem. Therefore, the tangential motion determined by (1.2) makes the evolving surface have minimal deformation rate (MDR). An advantage of this MDR formulation is that it can be coupled with the evolution equations of geometric quantities (such as normal vector and mean curvature) to provide stability, thereby proving convergence of evolving surface FEMs for closed evolving surfaces under many fundamental geometric flows. This has been shown for mean curvature flow and Willmore flow in [31] as well as surface evolution under a given velocity in [1]. However, the MDR formulation requires solving an additional evolution equation of normal vector n in convergence analysis and therefore requires higher smoothness of the initial surface in practical computation (see Figure 5 in Example 6.3). Convergence of finite element approximations to the MDR formulation of surface evolution by using normal vector of the numerically solved surface could not be proved so far.

In a recent article [18], Duan & Li proposed an artificial tangential motion which has minimal deformation energy (also known as the Dirichlet energy)

$$E_D[X(\cdot, t)] := \frac{1}{2} \int_{\Gamma^0} |\nabla_{\Gamma^0} X(\cdot, t)|^2 \tag{1.3}$$

under constraint $v \cdot n = u \cdot n$. This is equivalent to solving the following problem:

$$\begin{aligned} v \cdot n &= u \cdot n && \text{on } \Gamma(t) \\ -\Delta_{\Gamma^0} X &= \kappa \, (n \circ X) && \text{on } \Gamma^0, \end{aligned} \tag{1.4}$$

where $\kappa(\cdot, t) : \Gamma^0 \to \mathbb{R}$ represents a Lagrange multiplier arising from this constrained optimization problem. The minimal deformation (MD) formulation in (1.4) guarantees that the flow map $X(\cdot, t) : \Gamma^0 \to \Gamma(t)$ is a harmonic map with minimal deformation and therefore reduces mesh distortion caused by deformation. For genus-zero surfaces, harmonic map is equivalent to conformal map and therefore the flow map in the MD formulation maps triangles on Γ^0 to similar triangles on $\Gamma(t)$. However, the convergence of finite element approximations to surface evolution by the MD formulation remains an open and challenging problem.

The aim of this paper is to address the aforementioned challenges by proposing novel continuous formulation and evolving FEM which offer the following three advantages simultaneously:

- It contains an artificial tangential motion that could improve the mesh quality of evolving surfaces as effectively as the MD formulation in (1.4).
- It allows us to prove the convergence of finite element approximations to surface evolution with high-order accuracy.
- It avoids solving an additional evolution equation of n, which often causes the numerical solution of n to differ from the normal vector of the numerically-solved surface when the surface undergoes large deformation.

Through rigorous convergence analysis (for the second and third advantages) and numerical tests (for the first advantage) we find that a "relaxed" minimal deformation (RMD) formulation, which generates a tangential motion using harmonic map heat flow from Γ^0 to $\Gamma(t)$, has all the three advantages above.

At the continuous level, the RMD formulation seeks flow map $X(\cdot, t) : \Gamma^0 \to \Gamma(t)$, velocity $v(\cdot, t) : \Gamma^0 \to \mathbb{R}^3$ and an auxiliary function $\kappa(\cdot, t) : \Gamma^0 \to \mathbb{R}$ such that

$$\partial_t X = v \qquad \text{on } \Gamma^0 \tag{1.5a}$$

$$v \cdot (n \circ X) = (u \circ X) \cdot (n \circ X) \qquad \text{on } \Gamma^0 \tag{1.5b}$$

$$\partial_t X - \Delta_{\Gamma^0} X = \kappa \, (n \circ X) \qquad \text{on } \Gamma^0, \tag{1.5c}$$

where n denotes the normal vector on $\Gamma(t)$, and $n \circ X$ is the pull-back of n from $\Gamma(t)$ to Γ^0. An additional relaxation term, $\partial_t X$, is introduced to guarantee the convergence of finite element approximations. This is different from the DeTurck trick [37, 26] which uses harmonic map heat flow from Γ^0 to Γ^0 and solves non-divergence form of PDEs in local charts.

At the discrete level, we prove the convergence of semidiscrete finite element approximations to (1.5) for finite elements of degree $k \geq 4$. This restriction of finite elements degree is a technical requirement which ensures that the error of the numerical solution is sufficiently small in order to bound some nonlinear terms appearing in the error analysis; see the discussions in Section 7. In practical computation we observe that the evolving FEM based on the RMD formulation in (1.5) is also convergent for low-order finite elements of degree $k = 1, 2, 3$.

Our motivation for introducing the RMD formulation in (1.5), as well as the convergence analysis for finite element approximations of (1.5), is mainly based on the following three key observations. The first key observation is an intrinsic cancellation structure in the weak formulation of (1.5), i.e., orthogonality at the nodes that could exhibit a cancellation structure under the H^1 inner product (we refer readers to Lemma 3.8 for more details).

The second key observation is that the error equation for (1.5b) can be regarded as a discrete approximation to a hyperbolic transport equation, which allows us to establish an L^2-norm stability estimate for the normal component of the error by mimicking (at the discrete level) the stability estimates for hyperbolic transport equation; see the proof of Proposition 4.2.

The third key observation is that the presence of the relaxation term $\partial_t X$ in (1.5c) would lead to good estimates for the tangential component of the error. This observation about the role of relaxation term $\partial_t X$ for convergence analysis is also our motivation to consider the RMD formulation in (1.5).

The rest of this article is organized as follows. In Section 2, we introduce basic notations and the finite element scheme for approximating the surface evolution described by (1.5), and then present the main theorem on the convergence of numerical approximations. In Section 3, we introduce several important technical tools and techniques developed in [31, 32, 33, 34] and discuss about an important cancellation structure in the RMD formulation which allows us to prove convergence of numerical approximations in the presence of tangential motion. Stability of the numerical solutions is proved in Section 4, and error estimates are presented in Section 5. This completes the proof of the main theorem. In Section 6, we present several benchmark numerical examples to demonstrate the convergence of the proposed method and its advantages in improving the mesh quality of the approximate surfaces. Some conclusions and remarks are presented in Section 7. Some more details in the stability analysis are presented in Appendix.

2. Notations and main theorem

This section begins with an outline of basic notations in finite element approximations of surface evolution. Subsequently, we introduce the semidiscrete FEM for approximating surface evolution described by the RMD formulation in (1.5). Then we formulate the main theorem of this paper on the convergence of numerical approximations to surface evolution described by (1.5).

2.1. Basic notations

Let Γ be a smooth surface with the outward unit normal vector n. For a function $f : \Gamma \to \mathbb{R}$, its surface gradient on Γ is defined as a column vector $\nabla_\Gamma f = (I - nn^\top)(\nabla f^l)|_\Gamma$, where f^l is an arbitrary extension of f to $\mathbb{R}^3$ (the tangential gradient defined in this way is independent of the extension used to define it). The construction and associated differential-geometric notions can be found in [15] and Appendix A of [25], as well as in standard texts on differential geometry. For a column vector-valued function $f = (f_1, f_2, f_3)^\top : \Gamma \to \mathbb{R}^3$, its surface gradient is defined as a matrix $\nabla_\Gamma f = (\nabla_\Gamma f_1, \nabla_\Gamma f_2, \nabla_\Gamma f_3)$. For a matrix-valued function $P = (P_{i,j})_{1\le i,j\le 3} : \Gamma \to \mathbb{R}^{3\times 3}$, its surface gradient $\nabla_\Gamma P$ is a tensor with components $(\nabla_\Gamma P)_{ijk} = D_i(P_{j,k})$ for $1 \le i, k, j \le 3$.

An evolving surface $\Gamma(t)$, $t \in [0, T]$, with initial condition $\Gamma(0) = \Gamma^0$, can be described by a flow map $X : \Gamma^0 \times [0, T] \to \mathbb{R}^3$ which is diffeomorphic between Γ^0 and $\Gamma(t) = \{X(p, t) : p \in \Gamma^0\}$. For any function g defined on $\Gamma(t)$, we denote by $g(X)$ or $g \circ X$ the pullback function of g onto Γ^0.

Throughout this article, we denote by C and h_0 two generic positive constants which are different at different occurrences, possibly depending on the exact solution, the given velocity field u and T, but are independent of the mesh size h and $t \in [0, T]$. The notation $X \lesssim Y$ means $X \le CY$ for some constant C, and $X \sim Y$ means $X \lesssim Y$ and $Y \lesssim X$.

2.2. Evolving surface and finite element method

Given a closed, smooth initial surface $\Gamma^0 = \Gamma(0) \subset \mathbb{R}^3$, we denote by Γ_h^0 a piecewise curved triangular surface that interpolates Γ^0, with each piece of Γ_h^0 being the image of the reference plane triangle under a polynomial map of degree k; see [21, 17, 35]. Specifically, let $\Gamma_{h,f}^0$ be the piecewise flat triangular surface whose vertices coincide with those of Γ_h^0. Let K be a curved triangle on Γ_h^0, and let K_f be the corresponding flat triangle on $\Gamma_{h,f}^0$ with the same three vertices. Define $F_K : K_f \to K$ as the unique polynomial of degree k that parametrizes K. We assume that the initial triangulation is sufficiently good with the following property:

$$\max_{K\subset\Gamma_h^0} \left(\|F_K\|_{W^{k,\infty}(K_f)} + \|F_K^{-1}\|_{W^{1,\infty}(K)}\right) \lesssim 1, \tag{2.1}$$

where the right-hand side is independent of the mesh size h of the intepolated surface Γ_h^0. In particular, we assume that the given closed, smooth initial surface Γ^0 is partitioned into an admissible family of quasi-uniform triangulations with mesh size h.

We define a finite element space $S_h(\Gamma_h^0)$ of degree k on Γ_h^0 as

$$S_h(\Gamma_h^0) := \{v_h \in H^1(\Gamma_h^0) : v_h \circ F_K \in \mathbb{P}^k(K_f) \text{ for all } K \subset \Gamma_h^0\},$$

where $\mathbb{P}^k(K_f)$ denotes the space of polynomials of degree k on the flat triangle K_f.

Let $\mathbf{x}(0) = (x_1(0), \cdots, x_N(0)) \in \mathbb{R}^{3N}$ be the vector that collects all the finite element nodes $x_j(0)$ on Γ_h^0. Then we evolve vector $\mathbf{x}(0)$ in time and denote its position at time t by $\mathbf{x}(t) = (x_1(t), \cdots, x_N(t))$, which determines a surface $\Gamma_h(t) = \Gamma_h[\mathbf{x}(t)]$ by piecewise polynomial interpolation on the plane reference triangle. There exists a unique finite element function $X_h(\cdot, t) \in S_h(\Gamma_h^0)^3$ satisfying the following relations:

$$X_h\left(x_j(0), t\right) = x_j(t), \quad \forall j = 1, \ldots, N.$$

This is the discrete flow map which maps Γ_h^0 to $\Gamma_h[\mathbf{x}(t)]$. If $w(\cdot, t)$ is a function defined on $\Gamma_h[\mathbf{x}(t)]$ for $t \in [0, T]$, then the material derivative $\partial_{t,h}^\bullet w$ on $\Gamma_h[\mathbf{x}(t)]$ with respect to the discrete flow map X_h is defined by

$$\partial_{t,h}^\bullet w(x, t) = \frac{\mathrm{d}}{\mathrm{d}t} w\left(X_h(p, t), t\right) \text{ for } x = X_h(p, t) \in \Gamma_h[\mathbf{x}(t)].$$

The finite element basis functions on $\Gamma_h[\mathbf{x}(t)]$ are denoted by $\phi_j[\mathbf{x}(t)], j = 1, \ldots, N$, which satisfy the following identities:

$$\phi_j[\mathbf{x}(t)]\left(x_i(t)\right) = \delta_{ij}, \quad \partial_{t,h}^\bullet \phi_j[\mathbf{x}(t)] = 0, \quad i, j = 1, \ldots, N.$$

The pullback of $\phi_j[\mathbf{x}(t)]$ from any curved triangle on $\Gamma_h[\mathbf{x}(t)]$ to the reference plane triangle is a polynomial of degree k. The finite element space on the surface $\Gamma_h[\mathbf{x}(t)]$ is defined as

$$S_h(\Gamma_h[\mathbf{x}(t)]) := \mathrm{span}\{\phi_1[\mathbf{x}(t)], \cdots, \phi_N[\mathbf{x}(t)]\}.$$

The evolving surface FEM for (1.5) is to find $(X_h(\cdot, t), v_h(\cdot, t), \kappa_h(\cdot, t)) \in S_h(\Gamma_h^0)^3 \times S_h(\Gamma_h^0)^3 \times S_h(\Gamma_h^0)$ such that

$$\partial_t X_h = v_h \qquad \text{on } \Gamma_h^0, \tag{2.2a}$$

$$\int_{\Gamma_h^0} v_h \cdot \tilde{n}_h(X_h)\chi_n = \int_{\Gamma_h^0} u(X_h, t) \cdot \tilde{n}_h(X_h)\chi_n \qquad \forall \chi_n \in S_h(\Gamma_h^0), \tag{2.2b}$$

$$\int_{\Gamma_h^0} \partial_t X_h \cdot \chi_\kappa + \int_{\Gamma_h^0} \nabla_{\Gamma_h^0} X_h \cdot \nabla_{\Gamma_h^0} \chi_\kappa = \int_{\Gamma_h^0} \kappa_h \tilde{n}_h(X_h) \cdot \chi_\kappa \qquad \forall \chi_\kappa \in S_h(\Gamma_h^0)^3. \tag{2.2c}$$

where $\tilde{n}_h$ denotes the piecewisely defined normal vector on surface $\Gamma_h(t)$ (possibly discontinuous on the boundaries of the curved triangles), and $\tilde{n}_h(X_h)$ is its pullback to surface Γ_h^0. The initial condition for (2.2) is $X_h(\cdot, 0) = \mathrm{id}$ on Γ_h^0.

2.3. Interpolated surface and lifts

We denote by $X_h^*(\cdot, t) \in S_h(\Gamma_h^0)^3$ the interpolation of the exact flow map $X(\cdot, t) : \Gamma^0 \to \mathbb{R}^3$ that satisfies equation (1.5). This interpolated flow map can be expressed as

$$X_h^*(\cdot, t) := \sum_{j=1}^N x_j^*(t)\phi_j[\mathbf{x}(0)], \tag{2.3}$$

where the nodal vector $\mathbf{x}^*(t) = (x_1^*(t), \cdots, x_N^*(t))$ is determined by the exact flow map, i.e., $x_j^*(t) = X(x_j(0), t)$ for $j = 1, \ldots, N$. Then $X_h^*(\cdot, t)$ determines the interpolated surface $\Gamma_h[\mathbf{x}^*(t)]$, which is often abbreviated as $\Gamma_h^*(t)$ (in particular, $\Gamma_h^*(0) = \Gamma_h(0) = \Gamma_h^0$). We denote by $\tilde{n}_h^* = \tilde{n}_h^*(\cdot, t)$ the normal vector of the piecewise polynomial surface $\Gamma_h[\mathbf{x}^*(t)]$, which is discontinuous across the boundaries of the curved triangles on $\Gamma_h[\mathbf{x}^*(t)]$.

From [34, Lemma 7.1] or [17, (2.15)-(2.16)] we know that, for the smooth surface $\Gamma(t)$, there exists a constant h_0 such that for $h \le h_0$ and $t \in [0, T]$, any point $x \in \Gamma_h^*(t)$ can be lifted to $\Gamma(t)$ through a lift operator $a : \Gamma_h^*(t) \to \Gamma(t)$, i.e.,

$$x^l := a(x) \in \Gamma(t) \text{ for } x \in \Gamma_h^*(t). \tag{2.4}$$

The lift operator $a : \Gamma_h^*(t) \to \Gamma(t)$ is one-to-one and onto. Correspondingly, any function η on $\Gamma_h^*(t)$ can be lifted to a function η^l on $\Gamma(t)$, defined by

$$\eta^l(x^l) := \eta(x) \ \text{ for } \ x \in \Gamma_h^*(t).$$

The inverse lift of a function ϕ on $\Gamma(t)$ can be expressed as

$$\phi^{-l}(x) = \phi(x^l) \ \text{ for } \ x \in \Gamma_h^*(t).$$

Moreover, the L^2 and H^1 norms on $\Gamma_h^0 = \Gamma_h^*(0)$ and $\Gamma^0 = \Gamma(0)$ are equivalent, i.e.,

$$\begin{aligned} \|\eta\|_{L^2(\Gamma_h^0)} &\sim \|\eta^l\|_{L^2(\Gamma^0)} && \text{for } \ \eta \in L^2(\Gamma_h^0) \\ \|\nabla_{\Gamma_h^0}\eta\|_{L^2(\Gamma_h^0)} &\sim \|\nabla_{\Gamma^0}\eta^l\|_{L^2(\Gamma^0)} && \text{for } \ \eta \in H^1(\Gamma_h^0). \end{aligned} \tag{2.5}$$

2.4. Main theoretical result

We denote by $P_n : \Gamma^0 \to \mathbb{R}^{3\times 3}$ and $P_{\tan} : \Gamma^0 \to \mathbb{R}^{3\times 3}$ to be the normal and tangential projection matrices, i.e.,

$$P_n = (nn^\top) \circ X \quad \text{ and } \quad P_{\tan} = I_{3\times 3} - P_n, \tag{2.6}$$

where $n = n(\cdot, t)$ is the normal vector of $\Gamma(t)$. The main theoretical result of this article is the following theorem.

Theorem 2.1. *Let $u : \mathbb{R}^3 \times [0, T] \to \mathbb{R}^3$ be a given smooth velocity field, and assume that problem (1.5) admits a smooth solution (X, v, κ) such that the flow map $X(\cdot, t) : \Gamma^0 \to \Gamma(t)$ and its inverse map $X(\cdot, t)^{-1} : \Gamma(t) \to \Gamma^0$ are smooth for all $t \in [0, T]$. Then there exists a constant $h_0 > 0$ such that the finite element scheme in (2.2), with finite elements of polynomial degree $k \geq 4$, admits a unique finite element solution on the time interval $[0, T]$. Moreover, the finite element solution satisfies the following error bound for $0 < h \leq h_0$:*

$$\sup_{t\in[0,T]} \|(X_h)^l - X\|^2_{L^2(\Gamma^0)} + \int_0^T \|\nabla_{\Gamma^0} P_{\tan}((X_h)^l - X)\|^2_{L^2(\Gamma^0)} \mathrm{d}t \lesssim h^{2k}. \tag{2.7}$$

In Theorem 2.1, the gradient estimate applies only to the tangential component of the error. This is because the error estimate for the tangential part is derived from (2.2c), which includes a gradient term that enables us to obtain a gradient estimate for the tangential component (see Proposition 4.1 for further details). In contrast, the estimate for the normal component of the error is based on (2.2b), which only yields an L^2 estimate.

3. Basic tools for stability analysis

In this section, we present several fundamental tools for stability analysis. We begin by summarizing the notations and introducing the results of norm equivalence between different surfaces. Then we present results concerning the perturbation of normal vectors and characterize the difference between the normal vectors on different surfaces (i.e., the interpolated surface and the numerical-solution surface). This characterization plays a crucial role in the subsequent stability analysis. Finally, we illustrate an important cancellation structure in (2.2), another key to the stability analysis, by introducing the tangential and normal projections as well as utilizing the super-approximation properties.

3.1. Notations

We introduce $\Gamma_{h,\theta}(t)$ to denote the intermediate surface between the interpolated surface $\Gamma_h^*(t) = \Gamma_h[\mathbf{x}^*(t)]$ and the numerical solution surface $\Gamma_h(t) = \Gamma_h[\mathbf{x}(t)]$, defined as

$$\Gamma_{h,\theta}(t) := (1-\theta)\Gamma_h^*(t) + \theta\Gamma_h(t) = \Gamma_h[(1-\theta)\mathbf{x}^*(t) + \theta\mathbf{x}(t)], \quad \theta \in [0, 1]. \tag{3.1}$$

The flow map from Γ_h^0 to $\Gamma_{h,\theta}(t)$ is given by $X_h^\theta = (1-\theta)X_h^* + \theta X_h$, and the normal vector of $\Gamma_{h,\theta}(t)$ is denoted by $\tilde{n}_h^\theta = \tilde{n}_h^\theta(\cdot, t)$. For the readers' clarity and convenience, we summarize below the notations for functions on different surfaces, which will be frequently used in the stability analysis.

Γ^0:	The smooth initial surface at $t = 0$.
$X(\cdot, t)$:	The exact flow map defined on Γ^0, satisfying (1.5).
$\Gamma(t)$:	The exact surface determined by $X(\cdot, t)$ at time t.
Γ_h^0:	The piecewise curved triangular surface that interpolates Γ_0.
$X_h(\cdot, t)$:	The discrete flow map defined on Γ_h^0, satisfying (2.2).
$\Gamma_h(t)$:	The numerical-solution surface determined by $X_h(\cdot, t)$ at time t.
$X_h^*(\cdot, t)$:	The interpolation of $X(\cdot, t)$ defined on Γ_h^0, as given by (2.3).
$\Gamma_h^*(t)$:	The interpolated surface determined by $X_h^*(\cdot, t)$ at time t.
$\Gamma_{h,\theta}(t)$:	The intermediate surface between $\Gamma_h^*(t)$ and $\Gamma_h(t)$, as given by (3.1).
$X_h^\theta(\cdot, t)$:	The flow map from Γ_h^0 to $\Gamma_{h,\theta}(t)$.
n_{Γ^0}:	The normal vector on Γ^0.
$n, n_{\Gamma(t)}$:	The normal vector on $\Gamma(t)$.
P_n:	The normal projection matrix $P_n = (nn^\top) \circ X$, defined on Γ^0.
$P_{\tan}$:	The tangential projection matrix $P_{\tan} = I_{3\times 3} - P_n$, defined on Γ^0.
$n_{\Gamma_h^0}, H_{\Gamma_h^0}$:	The piecewisely defined normal vector and mean curvature on Γ_h^0.
$\tilde{n}_h$:	The piecewisely defined normal vector on surface $\Gamma_h(t)$.
$\tilde{n}_h^*, n_{\Gamma_h^*(t)}$:	The piecewisely defined normal vector on surface $\Gamma_h^*(t)$.
n_h^*:	The interpolation of n in $S_h(\Gamma_h^*(t))^3$, defined on $\Gamma_h^*(t)$, as given by (3.9).
P_n^*:	The normal projection matrix $P_n^* = \left(n_h^*(n_h^*)^\top\right) \circ X_h^*$, defined on Γ_h^0.
$P_{\tan}^*$:	The tangential projection matrix $P_{\tan}^* = I_{3\times 3} - P_n^*$, defined on Γ_h^0.
$\tilde{n}_h^\theta$:	The piecewisely defined normal vector on surface on $\Gamma_{h,\theta}(t)$.
I_h, P_{L^2}:	The Lagrange interpolation and the L^2-projection operators on $S_h(\Gamma_h^0)$.
v_h^*, κ_h^* :	The interpolation of the exact solution of (1.5), $v_h^* = I_h v^{(-l)}$ and $\kappa_h^* = I_h \kappa^{(-l)}$, defined on Γ_h^0.
e_X, e_v, e_κ :	The finite element error functions, $e_X = X_h - X_h^*$, $e_v = v_h - v_h^*$, and $e_\kappa = \kappa_h - \kappa_h^*$, defined on Γ_h^0.
e_n :	The error function of the normal vector, $e_n = \tilde{n}_h \circ X_h - n_h^* \circ X_h^*$ defined on Γ_h^0.
e_X^θ :	The finite element error function defined on $\Gamma_{h,\theta}(t)$ with the same nodal vector as e_X, as given by (3.2).
e_X^* :	The finite element error function defined on $\Gamma_h^*(t)$ with the same nodal vector as e_X, as given by (3.2).

3.2. Norm equivalence between different surfaces

We consider the norm equivalence relations between the interpolated surface $\Gamma_h^*(t) = \Gamma_h[\mathbf{x}^*(t)]$ and the numerical-solution surface $\Gamma_h(t) = \Gamma_h[\mathbf{x}(t)]$. Recall that $\Gamma_{h,\theta}(t)$ represents the intermediate surface between $\Gamma_h^*(t)$ and $\Gamma_h(t)$, as defined in (3.1).

Let $e_X = X_h - X_h^*$ be the finite element error function defined on Γ_h^0, and let $e_X^\theta = e_X \circ (X_h^\theta)^{-1}$ be the finite element function on $\Gamma_{h,\theta}(t)$ with the same nodal vector as e_X. In the case $\theta = 0$ we also write e_X^θ as e_X^*. If we denote by $\mathbf{e} = (e_1, \cdots, e_N)$, with $e_j = e_X(x_j(0), t)$ being the nodal values of the error function, then

$$
\begin{aligned}
e_X &= \sum_{j=1}^N e_j \phi_j[\mathbf{x}^*(0)] \in S_h(\Gamma_h^0)^3 && \text{on } \Gamma_h^0, \\
e_X^\theta &= \sum_{j=1}^N e_j \phi_j[\mathbf{x}^*(t) + \theta \mathbf{e}] \in S_h(\Gamma_{h,\theta}(t))^3 && \text{on } \Gamma_{h,\theta}(t), \\
e_X^* = e_X \circ (X_h^*)^{-1} &= \sum_{j=1}^N e_j \phi_j[\mathbf{x}^*(t)] \in S_h(\Gamma_h^*(t))^3 && \text{on } \Gamma_h^*(t).
\end{aligned} \tag{3.2}
$$

In general, a finite element function on $\Gamma_{h,\theta}(t)$ with nodal vector $\mathbf{w} = (w_1, \cdots, w_N)$ can be written as $w_h^\theta := \sum_{j=1}^N w_j \phi_j[\mathbf{x}^*(t) + \theta \mathbf{e}]$. The following theorem demonstrates that the norms on different intermediate surfaces $\Gamma_{h,\theta}(t)$ are actually equivalent to each other when the $W^{1,\infty}$ norm of e_X^* is bounded (see [32, Lemma 4.3] for more details).

Lemma 3.1 (Norm equivalence on $\Gamma_{h,\theta}$)**.** *If $\|\nabla_{\Gamma_h^*(t)} e_X^*\|_{L^\infty(\Gamma_h^*(t))} \le \frac{1}{2}$, then the following norm equivalence holds uniformly for $\theta \in [0,1]$ and $1 \le p \le \infty$:*

$$\|w_h^\theta\|_{L^p(\Gamma_{h,\theta}(t))} \lesssim \|w_h^0\|_{L^p(\Gamma_h^*(t))} \quad \textit{and} \quad \|\nabla_{\Gamma_{h,\theta}(t)} w_h^\theta\|_{L^p(\Gamma_{h,\theta}(t))} \lesssim \|\nabla_{\Gamma_h^*(t)} w_h^0\|_{L^p(\Gamma_h^*(t))}.$$

In addition, the norms of functions on Γ_h^0 and $\Gamma_h^*(t)$ (related to each other through the discrete flow map) are equivalent due to the boundedness of $X_h^*(\cdot,t)$ and $X_h^*(\cdot,t)^{-1}$ in the $W^{1,\infty}$ norm (this follows from the smoothness of flow map $X(\cdot,t)$ and its inverse $X(\cdot,t)^{-1}$ under the conditions of Theorem 2.1). We present this result in the following lemma.

Lemma 3.2 (Norm equivalence between Γ_h^0 and $\Gamma_h^*(t)$)**.** *For any function ϕ on Γ_h^0, we denote by $\phi^* = \phi \circ [X_h^*(\cdot,t)^{-1}]$ its push-forward function on $\Gamma_h^*(t)$ via the discrete flow map. Then, under the conditions of Theorem 2.1, there exists $h_0 > 0$ such that for $h \le h_0$ the following estimates hold*:

$$\begin{aligned} \|\phi^*\|_{L^p(\Gamma_h^*(t))} &\sim \|\phi\|_{L^p(\Gamma_h^0)} &\quad& \forall\, \phi \in L^p(\Gamma_h^0), \\ \|\nabla_{\Gamma_h^*(t)} \phi^*\|_{L^p(\Gamma_h^*(t))} &\sim \|\nabla_{\Gamma_h^0} \phi\|_{L^p(\Gamma_h^0)} && \forall\, \phi \in W^{1,p}(\Gamma_h^0). \end{aligned} \tag{3.3}$$

Proof. Since $\phi = \phi^* \circ X_h^*$, it follows that (applying the chain rule of partial differentiation)

$$\begin{aligned} \nabla_{\Gamma_h^0} \phi &= (\nabla_{\Gamma_h^0} X_h^*)[(\nabla_{\Gamma_h^*(t)} \phi^*) \circ X_h^*] \\ &= \big(\nabla_{\Gamma_h^0} X_h^* + n_{\Gamma_h^0} (n_{\Gamma_h^*(t)} \circ X_h^*)^\top\big)[(\nabla_{\Gamma_h^*(t)} \phi^*) \circ X_h^*], \end{aligned} \tag{3.4}$$

where $n_{\Gamma_h^0}$ and $n_{\Gamma_h^*(t)}$ denote the normal vectors of Γ_h^0 and $\Gamma_h^*(t)$, respectively, and the last equality follows from the orthogonality relation $n_{\Gamma_h^*(t)}^\top \nabla_{\Gamma_h^*(t)} \phi^* = 0$ on $\Gamma_h^*(t)$. Under the conditions of Theorem 2.1 (smoothness of the surface and the flow map), we have

$$\begin{aligned} \|(\nabla_{\Gamma_h^0} X_h^*) - (\nabla_{\Gamma^0} X)^{-l}\|_{L^\infty(\Gamma_h^0)} &\lesssim h^k \\ \|n_{\Gamma_h^0} (n_{\Gamma_h^*(t)} \circ X_h^*)^\top - (n_{\Gamma^0} (n_{\Gamma(t)} \circ X)^\top)^{-l}\|_{L^\infty(\Gamma_h^0)} &\lesssim h^k, \end{aligned} \tag{3.5}$$

which are standard estimates of errors related to an interpolation surface. Therefore, matrix $\nabla_{\Gamma_h^0} X_h^* + n_{\Gamma_h^0}(n_{\Gamma_h^*(t)} \circ X_h^*)^\top$ can be well approximated by matrix $\nabla_{\Gamma^0} X + n_{\Gamma^0}(n_{\Gamma(t)} \circ X)^\top$, while the latter matrix and its inverse matrix are bounded uniformly for $t \in [0,T]$. This implies that $\nabla_{\Gamma_h^0} X_h^* + n_{\Gamma_h^0}(n_{\Gamma_h^*(t)} \circ X_h^*)^\top$ and its inverse matrix are also bounded uniformly for $t \in [0,T]$. By a similar approach, the Jacobian matrix of the integral transformation from $\Gamma_h^*(t)$ to Γ_h^0 satisfies the property that $|\det(\nabla_{\Gamma_h^0} X_h^* (\nabla_{\Gamma_h^0} X_h^*)^\top + n_{\Gamma_h^0} (n_{\Gamma_h^0})^\top)|$ has both upper bound and positive lower bound. This immediately implies the norm equivalence relations in (3.3). $\square$

Remark 1 (Approximation of $\nabla_{\Gamma_h^0} X_h^* + n_{\Gamma_h^0}(n_{\Gamma_h^*(t)} \circ X_h^*)^\top$)**.** In the proof of Theorem 2.1, we often need to convert $\nabla_{\Gamma_h^*(t)}$ to $\nabla_{\Gamma_h^0}$, for which we need to use the chain rule of differentiation in (3.4), where the transition matrix $\nabla_{\Gamma_h^0} X_h^* + n_{\Gamma_h^0}(n_{\Gamma_h^*(t)} \circ X_h^*)^\top$ is discontinuous on the boundaries of the curved triangles on Γ_h^0. Nevertheless, as shown in the proof of Lemma 3.2, it can be well approximated by a continuous matrix $[\nabla_{\Gamma^0} X + n_{\Gamma^0}(n_{\Gamma(t)} \circ X)^\top]^{-l}$ with an error bound of $O(h^k)$.

The finite element scheme in (2.2) are defined on the discrete initial surface Γ_h^0, which is globally continuous and piecewise smooth. Special attention needs to be paid to the integration-by-parts argument on such piecewise smooth surfaces. To this end, we denote by $\mathcal{E}_h^0$ the collection of curved edges in the triangulated surface Γ_h^0, and present an integration-by-parts formula which involves jump terms on the curved edges of Γ_h^0.

Lemma 3.3 (Integration by parts on Γ_h^0)**.** *Let $v \in H^1(\Gamma_h^0)^3$ and $w \in H^1(\Gamma_h^0)$, for any fixed integer $k \ge 1$, there exists a constant $h_0 > 0$ such that for all mesh sizes satisfying $0 < h \le h_0$,* *it holds that,*

$$\Big|\int_{\Gamma_h^0} v\cdot\nabla_{\Gamma_h^0} w\Big| \lesssim \Big|\int_{\Gamma_h^0} (\nabla_{\Gamma_h^0}\cdot v)w\Big| + \|w\|_{L^2(\Gamma_h^0)}\|v\|_{L^2(\Gamma_h^0)} + h^k \sum_{E\in\mathcal{E}_h^0} \|w\|_{L^2(E)}\|v\|_{L^2(E)}. \quad (3.6)$$

Moreover, if v and w are finite element functions then

$$\Big|\int_{\Gamma_h^0} v\cdot\nabla_{\Gamma_h^0} w\Big| \lesssim \Big|\int_{\Gamma_h^0} (\nabla_{\Gamma_h^0}\cdot v)w\Big| + \|w\|_{L^2(\Gamma_h^0)}\|v\|_{L^2(\Gamma_h^0)}. \quad (3.7)$$

Proof. By using integration-by-parts on each curved triangle of Γ_h^0, and summing up the results for all the triangles, we can obtain

$$\int_{\Gamma_h^0} v\cdot\nabla_{\Gamma_h^0} w = \sum_{E\in\mathcal{E}_h^0}\int_E [\mu]_E\cdot v\,w + \int_{\Gamma_h^0} H_{\Gamma_h^0} n_{\Gamma_h^0}\cdot v\,w - \int_{\Gamma_h^0}(\nabla_{\Gamma_h^0}\cdot v)w, \quad (3.8)$$

where $n_{\Gamma_h^0}$ and $H_{\Gamma_h^0}$ are the normal vector and mean curvature of surface Γ_h^0, and $[\mu]_E$ denotes the jump of conormal vector on edge E. For $k=1$, the mean curvature $H_{\Gamma_h^0}$ is zero, and, for $k\geq 2$, based on Proposition 2.3 in [17], both the mean curvature $H_{\Gamma_h^0}$ and the normal vector $n_{\Gamma_h^0}$ converge to those of Γ^0 as the mesh size h tends to zero (with k fixed). Consequently, there exists a constant $h_0>0$ such that for all $0<h\leq h_0$,

$$\Big|\int_{\Gamma_h^0} H_{\Gamma_h^0} n_{\Gamma_h^0}\cdot v\,w\Big| \lesssim \|w\|_{L^2(\Gamma_h^0)}\|v\|_{L^2(\Gamma_h^0)}.$$

Moreover, on the interpolated surface Γ_h^0, it is well known that

$$\|[\mu]_E\|_{L^\infty(E)} \lesssim \|[n]_E\|_{L^\infty(E)} \lesssim h^k,$$

where $[n]_E$ denotes the jump of the normal vector across an edge E. This estimate is derived from (2.5) in [1] and Proposition 2.3 in [17]. Substituting those estimates into (3.8) immediately yields (3.6).

If v and w are finite element functions then the edge integrals in $h^k\sum_{E\in\mathcal{E}_h^0}\|w\|_{L^2(E)}\|v\|_{L^2(E)}$ can be reduced to surface integrals by using the trace inequality of finite element functions. This would reduce (3.6) to (3.7). ∎

3.3. Perturbation of normal vectors

Let $n_h^* = n_h^*(\cdot,t)\in S_h(\Gamma_h^*(t))^3$ denote the Lagrange interpolation of the normal vector $n=n(\cdot,t)$ of $\Gamma(t)$, given by

$$n_h^*(\cdot,t) := \sum_{j=1}^N n(x_j^*(t),t)\phi_j[\mathbf{x}^*(t)]. \quad (3.9)$$

It is noted that $n_h^*\in S_h(\Gamma_h^*(t))^3$ is continuous. This contrasts with the normal vectors $\tilde{n}_h$ of $\Gamma_h(t)$ and $\tilde{n}_h^*$ of $\Gamma_h^*(t)$, which are discontinuous on the boundaries of curved triangles. The error estimate between n_h^* and $\tilde{n}_h^*$ is well established and is presented in the following lemma, as stated in Proposition 2.3 of [17].

Lemma 3.4 (Approximation properties of n_h^* and $\tilde{n}_h^*$)**.** *Under the conditions of Theorem 2.1, the following estimates hold*:

$$\|n_h^*\circ X_h^* - (n\circ X)^{-l}\|_{L^\infty(\Gamma_h^0)} \lesssim h^{k+1}, \quad (3.10a)$$

$$\|\tilde{n}_h^*\circ X_h^* - (n\circ X)^{-l}\|_{L^\infty(\Gamma_h^0)} \lesssim h^{k}, \quad (3.10b)$$

$$\|\tilde{n}_h^*\circ X_h^* - n_h^*\circ X_h^*\|_{L^\infty(\Gamma_h^0)} \lesssim h^{k}. \quad (3.10c)$$

We now focus on estimating the difference between normal vectors $\tilde{n}_h$ of $\Gamma_h(t)$ and $\tilde{n}_h^*$ of $\Gamma_h^*(t)$. Before we present the result, we briefly recall that $\tilde{n}_h^\theta$ denotes the normal vector of the intermediate surface $\Gamma_{h,\theta}$, as defined in the text below (3.1), and e_X^* and e_X^θ are the error functions (with a common nodal vector) defined on the interpolated surface $\Gamma_h^*(t)$ and the intermediate surface $\Gamma_{h,\theta}$, respectively; see their definitions in (3.2).

Lemma 3.5 (Characterization of $\tilde n_h \circ X_h - \tilde n_h^* \circ X_h^*$)**.** *The following relation holds:*

$$\tilde n_h \circ X_h - \tilde n_h^* \circ X_h^* = -\int_0^1 [(\nabla_{\Gamma_{h,\theta}} e_X^\theta)\tilde n_h^\theta] \circ X_h^\theta \, \mathrm{d}\theta. \tag{3.11}$$

Moreover, by comparing $[(\nabla_{\Gamma_{h,\theta}} e_X^\theta)\tilde n_h^\theta] \circ X_h^\theta$ *with* $[(\nabla_{\Gamma_h^*} e_X^*)\tilde n_h^*] \circ X_h^*$ *using Newton–Leibniz formula with respect to* θ*, we have*

$$\begin{aligned}\tilde n_h \circ X_h - \tilde n_h^* \circ X_h^* &= \Big(-\nabla_{\Gamma_h^*(t)}(e_X^* \cdot n_h^*) + (\nabla_{\Gamma_h^*(t)} n_h^*) e_X^* + (\nabla_{\Gamma_h^*(t)} e_X^*)(n_h^* - \tilde n_h^*)\Big) \circ X_h^* \\ &\quad + \int_0^1 \Big(\int_0^\theta \Big(\big[2(\nabla_{\Gamma_{h,\alpha}} e_X^\alpha) - \tilde n_h^\alpha (\tilde n_h^\alpha)^\top (\nabla_{\Gamma_{h,\alpha}} e_X^\alpha)^\top\big] (\nabla_{\Gamma_{h,\alpha}} e_X^\alpha)\tilde n_h^\alpha \Big) \circ X_h^\alpha \, \mathrm{d}\alpha \Big) \mathrm{d}\theta.\end{aligned} \tag{3.12}$$

Proof. For a function w_h^θ on $\Gamma_{h,\theta}$, its material derivative in θ is defined as $(\partial_\theta^\bullet w_h^\theta)(X_h^\theta) := \frac{\mathrm{d}}{\mathrm{d}\theta}(w_h^\theta(X_h^\theta))$. The following expression of $\partial_\theta^\bullet \tilde n_h^\theta$ can be found in [13, Lemma 37]:

$$(\partial_\theta^\bullet \tilde n_h^\theta)(X_h^\theta) = \frac{\mathrm{d}}{\mathrm{d}\theta}(\tilde n_h^\theta \circ X_h^\theta) = -[(\nabla_{\Gamma_{h,\theta}} e_X^\theta)\tilde n_h^\theta] \circ X_h^\theta. \tag{3.13}$$

Then we note that relation (3.11) is an application of the Newton–Leibniz formula with the above expression of $\frac{\mathrm{d}}{\mathrm{d}\theta}(\tilde n_h^\theta \circ X_h^\theta)$. By using the Newton–Leibniz formula again, the right-hand side of (3.11) can be further written as

$$\begin{aligned}-\int_0^1 [(\nabla_{\Gamma_{h,\theta}} e_X^\theta)\tilde n_h^\theta] \circ X_h^\theta \, \mathrm{d}\theta &= -\,[(\nabla_{\Gamma_h^*(t)} e_X^*)\tilde n_h^*] \circ X_h^* \\ &\quad - \int_0^1 \Big(\int_0^\theta \big(\partial_\alpha^\bullet [(\nabla_{\Gamma_{h,\alpha}} e_X^\alpha)\tilde n_h^\alpha] \circ X_h^\alpha\big) \, \mathrm{d}\alpha \Big) \mathrm{d}\theta,\end{aligned} \tag{3.14}$$

where the first term on the right-hand side can be rewritten as follows, using the Leibniz rule of differentiation:

$$-(\nabla_{\Gamma_h^*(t)} e_X^*)\tilde n_h^* = -\nabla_{\Gamma_h^*(t)}(e_X^* \cdot n_h^*) + (\nabla_{\Gamma_h^*(t)} n_h^*) e_X^* + (\nabla_{\Gamma_h^*(t)} e_X^*)(n_h^* - \tilde n_h^*).$$

The second term on the right-hand side of (3.14) can also be rewritten into two terms, i.e.,

$$\begin{aligned}\partial_\alpha^\bullet [(\nabla_{\Gamma_{h,\alpha}} e_X^\alpha)\tilde n_h^\alpha] &= \partial_\alpha^\bullet (\nabla_{\Gamma_{h,\alpha}} e_X^\alpha)\tilde n_h^\alpha + (\nabla_{\Gamma_{h,\alpha}} e_X^\alpha)\partial_\alpha^\bullet \tilde n_h^\alpha \\ &= \partial_\alpha^\bullet (\nabla_{\Gamma_{h,\alpha}} e_X^\alpha)\tilde n_h^\alpha - (\nabla_{\Gamma_{h,\alpha}} e_X^\alpha)(\nabla_{\Gamma_{h,\alpha}} e_X^\alpha)\tilde n_h^\alpha,\end{aligned}$$

where the last equality follows from (3.13). We can further simplify the expression of $\partial_\alpha^\bullet(\nabla_{\Gamma_{h,\alpha}} e_X^\alpha)$ by using [24, Leamma 2.6], which says that

$$\partial_\alpha^\bullet(\nabla_{\Gamma_{h,\alpha}} e_X^\alpha) = \nabla_{\Gamma_{h,\alpha}}(\partial_\alpha^\bullet e_X^\alpha) - \Big(\nabla_{\Gamma_{h,\alpha}} e_X^\alpha - \tilde n_h^\alpha (\tilde n_h^\alpha)^\top (\nabla_{\Gamma_{h,\alpha}} e_X^\alpha)^\top\Big) (\nabla_{\Gamma_{h,\alpha}} e_X^\alpha).$$

In view of the expression of $\tilde n_h \circ X_h - \tilde n_h^* \circ X_h^*$ in (3.11), substituting $\partial_\alpha^\bullet e_X^\alpha = 0$ and the above three relations into (3.14) yields (3.12). ☐

We are now ready to define the normal projection matrix $P_n^* \in H^1(\Gamma_h^0, \mathbb{R}^{3\times 3})$ and tangential projection matrix $P_{\tan}^* \in H^1(\Gamma_h^0, \mathbb{R}^{3\times 3})$ on the discrete surface Γ_h^0, i.e.,

$$P_n^* = \big(n_h^* (n_h^*)^\top\big) \circ X_h^* \quad \text{and} \quad P_{\tan}^* = I_{3\times 3} - P_n^*, \tag{3.15}$$

where n_h^* is the (globally continuous) interpolated normal vector on the interpolated surface $\Gamma_h^*(t)$. The gradient of the normal projection matrix, i.e., $\nabla_{\Gamma_h^0} P_n^*$, is defined as a third-order tensor. While it is discontinuous on Γ_h^0, it can be approximated by a continuous tensor $(\nabla_{\Gamma^0} P_n)^{-l}$, where P_n is defined in (2.6). In particular, $(\nabla_{\Gamma_h^0} P_n^*) - (\nabla_{\Gamma^0} P_n)^{-l}$ has the same error bound as $n_h^* - n^{-l}$. This is presented in the following lemma.

Lemma 3.6 (Approximation of $\nabla_{\Gamma_h^0} P_n^*$)**.** *Under the conditions of Theorem 2.1, it holds that*

$$\|(\nabla_{\Gamma_h^0} P_n^*) - (\nabla_{\Gamma^0} P_n)^{-l}\|_{L^\infty(\Gamma_h^0)} \lesssim h^k. \tag{3.16}$$

Since our numerical scheme and error analysis are conducted on Γ_h^0, we typically need to pull the normal vectors of $\Gamma_h(t)$ and $\Gamma_h^*(t)$ back to Γ_h^0, denoted by $\tilde{n}_h \circ X_h, \tilde{n}_h^* \circ X_h^*$, and $n_h^* \circ X_h^*$, respectively. Therefore, for the simplicity of notation, we abbreviate them as $\tilde{n}_h, \tilde{n}_h^*$, and n_h^* (omitting the composition with flow maps), respectively, in the subsequent text when it does not cause ambiguity.

3.4. Cancellation structure

Let I_h and P_{L^2} be the Lagrange interpolation and the L^2-projection operators on $S_h(\Gamma_h^0)$, respectively, and recall that P_n^* and $P_{\tan}^* \in H^1(\Gamma_h^0)^{3\times 3}$ are the normal projection matrix and tangential projection matrix defined in (3.15). For any $w_h \in S_h(\Gamma_h^0)^3$, we define $I_h(P_n^* w_h)$ and $P_{L^2}(P_n^* w_h)$ as the interpolated and projected normal components of w_h, respectively. They are finite element functions in $S_h(\Gamma_h^0)^3$ such that the differences $P_n^* w_h - I_h(P_n^* w_h)$ and $P_n^* w_h - P_{L^2}(P_n^* w_h)$ have better estimates than the usual results, as shown in Lemma 3.7. These better estimates are referred to as super-approximation properties, which are frequently used in this paper and summarized in the following lemma. We direct readers to [31, Lemma A] for further details.

Lemma 3.7 (Super-approximation properties)**.** *For any $w_h \in S_h(\Gamma_h^0)^3$, under the condition of Theorem 2.1, the following inequalities hold*:

$$
\begin{aligned}
\|P_n^* w_h - I_h(P_n^* w_h)\|_{L^2(\Gamma_h^0)} &\lesssim h^2 \|w_h\|_{H^1(\Gamma_h^0)}, \\
\|\nabla_{\Gamma_h^0}(P_n^* w_h) - \nabla_{\Gamma_h^0} I_h(P_n^* w_h)\|_{L^2(\Gamma_h^0)} &\lesssim h \|w_h\|_{H^1(\Gamma_h^0)}, \\
\|P_n^* w_h - P_{L^2}(P_n^* w_h)\|_{L^2(\Gamma_h^0)} &\lesssim h^2 \|w_h\|_{H^1(\Gamma_h^0)}, \\
\|\nabla_{\Gamma_h^0}(P_n^* w_h) - \nabla_{\Gamma_h^0} P_{L^2}(P_n^* w_h)\|_{L^2(\Gamma_h^0)} &\lesssim h \|w_h\|_{H^1(\Gamma_h^0)}.
\end{aligned}
$$

Similar estimates also hold for $P_{\tan}^* w_h - I_h(P_{\tan}^* w_h)$ and $P_{\tan}^* w_h - P_{L^2}(P_{\tan}^* w_h)$.

By utilizing the super-approximation properties, we illustrate a cancellation structure between the normal projection and the tangential projection in the weak formulation (2.2), which is crucial to proving convergence of the evolving FEM in this paper.

Lemma 3.8 (Cancellation structure)**.** *Under the conditions of Theorem 2.1, the following estimates hold for any $w_h, z_h \in S_h(\Gamma_h^0)^3$ (which are possibly time-dependent)*:

$$
\int_{\Gamma_h^0} \nabla_{\Gamma_h^0}(P_n^* w_h) \cdot \nabla_{\Gamma_h^0}(I_h P_{\tan}^* z_h) \lesssim \|w_h\|_{L^2(\Gamma_h^0)} \big(\|z_h\|_{L^2(\Gamma_h^0)} + \|\nabla_{\Gamma_h^0}(P_{\tan}^* z_h)\|_{L^2(\Gamma_h^0)}\big), \tag{3.17}
$$

$$
\begin{aligned}
\int_{\Gamma_h^0} \partial_t(P_n^* w_h) \cdot (I_h P_{\tan}^* z_h) \lesssim{}& \|w_h\|_{L^2(\Gamma_h^0)} \|z_h\|_{L^2(\Gamma_h^0)} \\
&+ h^2 \|\partial_t w_h\|_{L^2(\Gamma_h^0)} (\|z_h\|_{L^2(\Gamma_h^0)} + \|\nabla_{\Gamma_h^0}(P_{\tan}^* z_h)\|_{L^2(\Gamma_h^0)}).
\end{aligned} \tag{3.18}
$$

Remark 2. Compared with the usual estimates without making use of the orthogonality between P_n^* and $P_{\tan}^*$, the right-hand sides of (3.17) and (3.18) have either weaker norms or some power of h. This is the reason that we refer to them as cancellation structure.

Proof. Due to the orthogonality between P_n^* and $P_{\tan}^*$, it is easy to see that $I_h P_n^* \phi_h = 0$ for the function $\phi_h = I_h P_{\tan}^* z_h$ (simply verify that $I_h P_n^* \phi_h = 0$ at the nodes). For this function ϕ_h, using Lemma 3.7 (super-approximation properties), we have

$$
\|\nabla_{\Gamma_h^0}(P_n^* \phi_h)\|_{L^2(\Gamma_h^0)} = \|\nabla_{\Gamma_h^0}(P_n^* \phi_h - I_h(P_n^* \phi_h))\|_{L^2(\Gamma_h^0)} \lesssim h \|\phi_h\|_{H^1(\Gamma_h^0)}. \tag{3.19}
$$

By applying the Leibniz rule of differentiation, we have

$$
\begin{aligned}
\int_{\Gamma_h^0} \nabla_{\Gamma_h^0}(P_n^* w_h) \cdot \nabla_{\Gamma_h^0} \phi_h &= \int_{\Gamma_h^0} \nabla_{\Gamma_h^0} w_h \cdot \nabla_{\Gamma_h^0}(P_n^* \phi_h) + \int_{\Gamma_h^0} (\nabla_{\Gamma_h^0} P_n^*) w_h \cdot \nabla_{\Gamma_h^0} \phi_h \\
&\quad - \int_{\Gamma_h^0} \nabla_{\Gamma_h^0} w_h \cdot (\nabla_{\Gamma_h^0} P_n^*) \phi_h \\
&=: I_1 + I_2 - I_3,
\end{aligned} \tag{3.20}
$$

where I_1 can be estimated directly using (3.19), i.e.,

$$|I_1| \lesssim \|\nabla_{\Gamma_h^0} w_h\|_{L^2(\Gamma_h^0)} h \|\phi_h\|_{H^1(\Gamma_h^0)} \lesssim \|w_h\|_{L^2(\Gamma_h^0)} \|\phi_h\|_{H^1(\Gamma_h^0)}.$$

Moreover, I_2 can be estimated directly with the boundedness of $\|\nabla_{\Gamma_h^0} P_n^*\|_{L^\infty(\Gamma_h^0)}$, i.e.,

$$|I_2| \lesssim \|w_h\|_{L^2(\Gamma_h^0)} \|\nabla_{\Gamma_h^0} \phi_h\|_{L^2(\Gamma_h^0)}.$$

The following estimate of I_3 can be obtained through approximating $\nabla_{\Gamma_h^0} P_n^*$ by $(\nabla_{\Gamma^0} P_n)^{-l}$ using Lemma 3.6 and the inverse inequality $\|\nabla_{\Gamma_h^0} w_h\|_{L^2(\Gamma_h^0)} \le Ch^{-1} \|w_h\|_{L^2(\Gamma_h^0)}$:

$$|I_3| \le \Big| \int_{\Gamma_h^0} \nabla_{\Gamma_h^0} w_h \cdot (\nabla_{\Gamma^0} P_n)^{-l} \phi_h \Big| + Ch^{k-1} \|w_h\|_{L^2(\Gamma_h^0)} \|\phi_h\|_{L^2(\Gamma_h^0)}.$$

Then we can employ the integration by parts to transfer the gradient from w_h to ϕ_h. We apply the integration-by-parts estimate in (3.6) of Lemma 3.3 with $v = (\nabla_{\Gamma^0} P_n)^{-l} \phi_h$, and use inverse inequality to reduce the edge integrals in (3.6) to surface integrals similarly as (3.7) of Lemma 3.3. This leads to the following result (note that $\|\nabla_{\Gamma_h^0} \cdot v\|_{L^2(\Gamma_h^0)} \lesssim \|\phi_h\|_{H^1(\Gamma_h^0)}$):

$$|I_3| \lesssim \|w_h\|_{L^2(\Gamma_h^0)} (\|\phi_h\|_{L^2(\Gamma_h^0)} + \|\nabla_{\Gamma_h^0} \phi_h\|_{L^2(\Gamma_h^0)}).$$

Therefore, substituting the estimates of I_1, I_2 and I_3 into (3.20) and recalling that $\phi_h = I_h P_{\tan}^* z_h$, we have

$$\begin{aligned} \int_{\Gamma_h^0} \nabla_{\Gamma_h^0} (P_n^* w_h) \cdot \nabla_{\Gamma_h^0} (I_h P_{\tan}^* z_h) &\lesssim \|w_h\|_{L^2(\Gamma_h^0)} (\|\phi_h\|_{L^2(\Gamma_h^0)} + \|\nabla_{\Gamma_h^0} \phi_h\|_{L^2(\Gamma_h^0)}) \\ &\lesssim \|w_h\|_{L^2(\Gamma_h^0)} \big(\|z_h\|_{L^2(\Gamma_h^0)} + \|\nabla_{\Gamma_h^0} (P_{\tan}^* z_h)\|_{L^2(\Gamma_h^0)} \big), \end{aligned} \tag{3.21}$$

where the last inequality follows from approximating $I_h P_{\tan}^* z_h$ by $P_{\tan}^* z_h$ with the super-approximation properties in Lemma 3.7. This proves the first result of Lemma 3.8.

The second result of Lemma 3.8 can be proved similarly, utilizing the orthogonality between P_n^* and $P_{\tan}^*$, as well as the super-approximation properties in Lemma 3.7. The former guarantees that $I_h P_n^* \phi_h = I_h P_n^* (I_h P_{\tan}^* z_h) = 0$ and the latter guarantees the following estimate:

$$\|P_n^* \phi_h\|_{L^2(\Gamma_h^0)} = \|P_n^* \phi_h - I_h P_n^* \phi_h\|_{L^2(\Gamma_h^0)} \lesssim h^2 \|\phi_h\|_{H^1(\Gamma_h^0)}.$$

Therefore,

$$\begin{aligned} \int_{\Gamma_h^0} \partial_t (P_n^* w_h) \cdot \phi_h &= \int_{\Gamma_h^0} (\partial_t P_n^*) w_h \cdot \phi_h + \partial_t w_h \cdot (P_n^* \phi_h) \\ &\lesssim \|w_h\|_{L^2(\Gamma_h^0)} \|\phi_h\|_{L^2(\Gamma_h^0)} + \|\partial_t w_h\|_{L^2(\Gamma_h^0)} \|P_n^* \phi_h\|_{L^2(\Gamma_h^0)} \\ &\lesssim \|w_h\|_{L^2(\Gamma_h^0)} \|z_h\|_{L^2(\Gamma_h^0)} + h^2 \|\partial_t w_h\|_{L^2(\Gamma_h^0)} \|\phi_h\|_{H^1(\Gamma_h^0)}. \end{aligned}$$

Since $\|\phi_h\|_{H^1(\Gamma_h^0)} \lesssim \|z_h\|_{L^2(\Gamma_h^0)} + \|\nabla_{\Gamma_h^0} (P_{\tan}^* z_h)\|_{L^2(\Gamma_h^0)}$, as shown in (3.21) for $\phi_h = I_h P_{\tan}^* z_h$, the above estimate gives the second result of Lemma 3.8. □

4. Stability estimates

4.1. Error equations and defects

We denote by $(X_h^*, v_h^*, \kappa_h^*) \in S_h(\Gamma_h^0)^3 \times S_h(\Gamma_h^0)^3 \times S_h(\Gamma_h^0)$ the interpolation of the exact solution (X, v, κ), and recall that $n_h^* \in S_h(\Gamma_h^*(t))^3$ denotes the interpolation of normal vector n on $\Gamma(t)$. Replacing $(X_h, v_h, \kappa_h, \tilde{n}_h)$ by $(X_h^*, v_h^*, \kappa_h^*, n_h^*)$ in weak formulation (2.2), we can obtain a weak formulation satisfied by X_h^*, v_h^*, κ_h^* and n_h^* up to some defects, i.e.,

$$\partial_t X_h^* = v_h^* \qquad \text{on } \Gamma_h^0, \tag{4.1a}$$

$$\int_{\Gamma_h^0} v_h^* \cdot n_h^*(X_h^*) \chi_n = \int_{\Gamma_h^0} u(X_h^*, t) \cdot n_h^*(X_h^*) \chi_n - \int_{\Gamma_h^0} d_v \chi_n \qquad \forall \chi_n \in S_h(\Gamma_h^0), \tag{4.1b}$$

$$\int_{\Gamma_h^0} \partial_t X_h^* \chi_\kappa + \int_{\Gamma_h^0} \nabla_{\Gamma_h^0} X_h^* \nabla_{\Gamma_h^0} \chi_\kappa = \int_{\Gamma_h^0} \kappa_h^* n_h^*(X_h^*) \cdot \chi_\kappa - \int_{\Gamma_h^0} d_\kappa \cdot \chi_\kappa \quad \forall \chi_\kappa \in S_h(\Gamma_h^0)^3, \tag{4.1c}$$

where $d_v(\cdot,t) \in S_h(\Gamma_h^0)$ and $d_\kappa(\cdot,t) \in S_h(\Gamma_h^0)^3$ are the defects due to spatial discretization. In the following error analysis, we need to estimate the defect function $d_\kappa \in S_h(\Gamma_h^0)^3$ in both L^2 norm and the discrete H^{-1} norm. The latter is defined as

$$\|d_\kappa\|_{H_h^{-1}(\Gamma_h^0)} = \sup_{0\neq\phi_h\in S_h(\Gamma_h^0)^3} \frac{\int_{\Gamma_h^0} d_\kappa \phi_h}{\|\phi_h\|_{H^1(\Gamma_h^0)}}. \tag{4.2}$$

Upon subtracting equations (4.1) from equations (2.2), we derive the following error equations for $e_X = X_h - X_h^* \in S_h(\Gamma_h^0)^3$, $e_v = v_h - v_h^* \in S_h(\Gamma_h^0)^3$ and $e_\kappa := \kappa_h - \kappa_h^* \in S_h(\Gamma_h^0)$:

$$\partial_t e_X = e_v, \quad \text{on } \Gamma_h^0, \tag{4.3a}$$

$$\int_{\Gamma_h^0} (v_h \cdot \tilde n_h(X_h) - v_h^* \cdot n_h^*(X_h^*))\chi_n = \int_{\Gamma_h^0} ((u\cdot \tilde n_h)(X_h) - (u\cdot n_h^*)(X_h^*))\chi_n + \int_{\Gamma_h^0} d_v \chi_n, \tag{4.3b}$$

$$\int_{\Gamma_h^0} \partial_t e_X \chi_\kappa + \int_{\Gamma_h^0} \nabla_{\Gamma_h^0} e_X \nabla_{\Gamma_h^0}\chi_\kappa = \int_{\Gamma_h^0} (\kappa_h \tilde n_h(X_h) - \kappa_h^* n_h^*(X_h^*))\chi_\kappa + \int_{\Gamma_h^0} d_\kappa \chi_\kappa. \tag{4.3c}$$

Additionally, we denote by $e_n := \tilde n_h \circ X_h - n_h^* \circ X_h^*$ on Γ_h^0 the error of the normal vector. The stability analysis will be based on the error equations in (4.3).

4.2. Time derivative of the error

Let $t^* \in (0,T]$ be the supremum of time such that the finite element scheme in (2.2) has a unique finite element solution satisfying the following estimate (with coefficient 1 on the right-hand side):

$$\|e_X(\cdot,t)\|_{L^2(\Gamma_h^0)} \le h^{k-0.1}, \quad \text{for} \quad t\in[0,t^*]. \tag{4.4}$$

The choice of 0.1 in the exponent is not essential to the analysis, as any small positive number $0<\epsilon<1$ would suffice for the following proof. Since $e_X(\cdot,0)=0$ and the semidiscrete finite element solution of (2.2) is continuous in time, it follows that $t^*>0$. Ultimately, our proof will be completed by demonstrating that $t^*=T$.

Given condition $k\ge 4$ and the inverse inequality $\|e_X(\cdot,t)\|_{W^{1,\infty}(\Gamma_h^0)} \le Ch^{-2}\|e_X(\cdot,t)\|_{L^2(\Gamma_h^0)}$, (4.4) implies the boundedness of $X_h(\cdot,t)$ and smallness of e_X in the $W^{1,\infty}$ norm for $t\in[0,t^*]$. For sufficiently small h (smaller than some constant), Lemma 3.2 (norm equivalence between Γ_h^0 and $\Gamma_h^*(t)$) implies that, for $e_X^* = e_X \circ (X_h^*)^{-1}$,

$$\|\nabla_{\Gamma_h^*(t)} e_X^*\|_{L^\infty(\Gamma_h^*(t))} \sim \|\nabla_{\Gamma_h^0} e_X\|_{L^\infty(\Gamma_h^0)} \lesssim h^{-2}\|e_X\|_{L^2(\Gamma_h^0)} \lesssim h^{k-2.1} \le \frac12. \tag{4.5}$$

Therefore, Lemma 3.1 (norm equivalence on $\Gamma_{h,\theta}$) holds for $t\in[0,t^*]$.

Lemma 4.1 (Estimates of e_n)**.** *Under the conditions of Theorem 2.1 and (4.4), the following estimates hold for $t\in[0,t^*]$:*

$$\|e_n\|_{L^2(\Gamma_h^0)} \lesssim h^{-1}\|e_X\|_{L^2(\Gamma_h^0)} + h^k \quad \textit{and} \quad \|e_n\|_{L^\infty(\Gamma_h^0)} \lesssim h^{-1}\|e_X\|_{L^\infty(\Gamma_h^0)} + h^k. \tag{4.6}$$

Proof. The estimates in (4.6) are consequences of formula (3.11) in Lemma 3.5, which implies that

$$\|\tilde n_h \circ X_h - \tilde n_h^* \circ X_h^*\|_{L^2(\Gamma_h^0)} \lesssim h^{-1}\|e_X\|_{L^p(\Gamma_h^0)} \quad \text{for } 2\le p\le\infty.$$

This, together with $\|\tilde n_h^* - n_h^*\|_{L^\infty(\Gamma_h^*(t))} \lesssim h^k$ and $e_n = \tilde n_h\circ X_h - n_h^*\circ X_h^*$, implies (4.6). □

A direct application of Lemma 4.1, in combination with (4.4), is the following result:

$$\|e_n\|_{L^2(\Gamma_h^0)} \lesssim h^{k-1.1} \quad \text{and} \quad \|e_n\|_{L^\infty(\Gamma_h^0)} \lesssim h^{k-2.1} \quad \text{for } t\in[0,t^*]. \tag{4.7}$$

Both (4.4) and (4.7) will be frequently used in the subsequent stability analysis.

We are now ready to estimate the time derivative of the error, i.e., $e_v = \partial_t e_X$. We start with presenting a rough estimate and then improve the result by decomposing $\partial_t e_X$ into $\partial_t(P_{\tan}^* e_X)$ and $\partial_t[e_X\cdot(n_h^*\circ X_h^*)]$, and applying Lemma 3.8 (cancellation structure).

Lemma 4.2 (A rough estimate of $\partial_t e_X$)**.** *Under the conditions of Theorem 2.1, the following estimate holds for* $t \in [0, t^*]$:

$$\|\partial_t e_X\|_{L^2(\Gamma_h^0)} \lesssim h^{-2}\|e_X\|_{L^2(\Gamma_h^0)} + \|e_\kappa\|_{L^2(\Gamma_h^0)} + \|d_\kappa\|_{L^2(\Gamma_h^0)} + h^k. \tag{4.8}$$

Proof. Choosing $\chi_\kappa := \partial_t e_X$ as the test function in weak formulation (4.3c), we have

$$\begin{aligned}\|\partial_t e_X\|^2_{L^2(\Gamma_h^0)} &= -\int_{\Gamma_h^0} \nabla_{\Gamma_h^0} e_X \nabla_{\Gamma_h^0} \partial_t e_X + \int_{\Gamma_h^0} (e_\kappa \tilde{n}_h + \kappa_h^* e_n) \cdot \partial_t e_X + \int_{\Gamma_h^0} d_\kappa \cdot \partial_t e_X \\ &\lesssim \big(h^{-2}\|e_X\|_{L^2(\Gamma_h^0)} + \|e_\kappa\|_{L^2(\Gamma_h^0)} + \|e_n\|_{L^2(\Gamma_h^0)} + \|d_\kappa\|_{L^2(\Gamma_h^0)}\big)\|\partial_t e_X\|_{L^2(\Gamma_h^0)},\end{aligned}$$

where the inverse inequality $\|\nabla_{\Gamma_h^0} v_h\|_{L^2(\Gamma_h^0)} \le C\, h^{-1}\|v_h\|_{L^2(\Gamma_h^0)}$ is used with $v_h = e_X$ and $v_h = \partial_t e_X$, respectively. Then (4.8) follows from applying Lemma 4.1. □

Then, by choosing test function $\chi_\kappa = I_h P^*_{\tan}\phi_h$ in weak formulation (4.3c), we can derive the following estimate of $\partial_t P^*_{\tan} e_X$. We refer to Appendix A for more details.

Lemma 4.3 (Estimate of $\partial_t P^*_{\tan} e_X$)**.** *Under the conditions of Theorem 2.1, the following estimate holds for* $t \in [0, t^*]$:

$$\begin{aligned}\|\partial_t P^*_{\tan} e_X\|_{L^2(\Gamma_h^0)} \lesssim h^{-1}\big(&\|\nabla_{\Gamma_h^0} P^*_{\tan} e_X\|_{L^2(\Gamma_h^0)} + \|e_X\|_{L^2(\Gamma_h^0)}\big) \\ &+ h\|e_\kappa\|_{L^2(\Gamma_h^0)} + \|d_\kappa\|_{L^2(\Gamma_h^0)} + h^k.\end{aligned} \tag{4.9}$$

Similarly, by choosing test function $\chi_n := P_{L^2}\partial_t[e_X \cdot (n_h^* \circ X_h^*)]$ in weak formulation (4.3b), we can derive the following estimate of $\partial_t[e_X \cdot (n_h^* \circ X_h^*)]$; see Appendix B for more details.

Lemma 4.4 (Estimate of $\partial_t[e_X \cdot (n_h^* \circ X_h^*)]$)**.** *Under the conditions of Theorem 2.1, the following estimate holds for* $t \in [0, t^*]$:

$$\begin{aligned}\|\partial_t[e_X \cdot (n_h^* \circ X_h^*)]\|_{L^2(\Gamma_h^0)} \lesssim h^{-1}&\|e_X\|_{L^2(\Gamma_h^0)} + h\|e_\kappa\|_{L^2(\Gamma_h^0)} \\ &+ h\|d_\kappa\|_{L^2(\Gamma_h^0)} + \|d_v\|_{L^2(\Gamma_h^0)} + h^k.\end{aligned} \tag{4.10}$$

Lemma 4.5 (Estimate of e_κ)**.** *Under the conditions of Theorem 2.1, the following estimate holds for* $t \in [0, t^*]$:

$$\|e_\kappa\|_{L^2(\Gamma_h^0)} \lesssim h^{-2}\|e_X\|_{L^2(\Gamma_h^0)} + \|d_\kappa\|_{L^2(\Gamma_h^0)} + \|d_v\|_{L^2(\Gamma_h^0)} + h^k, \tag{4.11}$$

for sufficiently small $h \le h_0$.

Proof. For the simplicity of notation, we abbreviate $n_h^* \circ X_h^*$ as n_h^* here. In view of (3.10a) in Lemma 3.4 (approximation properties of n_h^* and $\tilde{n}_h^*$), we have

$$\big|\|e_\kappa\|^2_{L^2(\Gamma_h^0)} - \|e_\kappa n_h^*\|^2_{L^2(\Gamma_h^0)}\big| \le \|e_\kappa\|^2_{L^2(\Gamma_h^0)}\||n_h^*|^2 - 1\|_{L^\infty(\Gamma_h^0)} \lesssim h^{k+1}\|e_\kappa\|^2_{L^2(\Gamma_h^0)}.$$

This implies the following equivalence of norms:

$$\|e_\kappa\|_{L^2(\Gamma_h^0)} \sim \|e_\kappa n_h^*\|_{L^2(\Gamma_h^0)}. \tag{4.12}$$

Then, choosing test function $\chi_\kappa := P_{L^2}(e_\kappa n_h^*)$ in the weak formulation (4.3c), we obtain

$$\begin{aligned}\|e_\kappa n_h^*\|^2_{L^2(\Gamma_h^0)} &= \int_{\Gamma_h^0} e_\kappa n_h^* \cdot (e_\kappa n_h^* - P_{L^2}(e_\kappa n_h^*)) - \int_{\Gamma_h^0} \kappa_h^* e_n \cdot P_{L^2}(e_\kappa n_h^*) \\ &- \int_{\Gamma_h^0} e_\kappa e_n \cdot P_{L^2}(e_\kappa n_h^*) - \int_{\Gamma_h^0} d_\kappa \cdot P_{L^2}(e_\kappa n_h^*) + \int_{\Gamma_h^0} \partial_t e_X \cdot P_{L^2}(e_\kappa n_h^*) \\ &+ \int_{\Gamma_h^0} \nabla_{\Gamma_h^0} e_X \cdot \nabla_{\Gamma_h^0} P_{L^2}(e_\kappa n_h^*),\end{aligned}$$

from which we can derive the result of Lemma 4.5; see Appendix C for more details. □

Remark 3 (An improved estimate of e_v)**.** In summary, by combining Lemma 4.3 (estimate of $\partial_t P^*_{\tan} e_X$), Lemma 4.4 (estimate of $\partial_t[e_X \cdot (n_h^* \circ X_h^*)]$) and Lemma 4.5 (estimate of e_κ), we can obtain the following results:

$$\|\partial_t P^*_{\tan} e_X\|_{L^2(\Gamma_h^0)} \lesssim h^{-1}\big(\|\nabla_{\Gamma_h^0} P^*_{\tan} e_X\|_{L^2(\Gamma_h^0)} + \|e_X\|_{L^2(\Gamma_h^0)}\big)$$

$$+\|d_\kappa\|_{L^2(\Gamma_h^0)}+h\|d_v\|_{L^2(\Gamma_h^0)}+h^k, \tag{4.13}$$

$$\|\partial_t[e_X\cdot(n_h^*\circ X_h^*)]\|_{L^2(\Gamma_h^0)}\lesssim h^{-1}\|e_X\|_{L^2(\Gamma_h^0)}+h\|d_\kappa\|_{L^2(\Gamma_h^0)}+\|d_v\|_{L^2(\Gamma_h^0)}+h^k. \tag{4.14}$$

Compared with Lemma 4.2, the following improved estimate of $e_v=\partial_t e_X$ can be shown:

$$\begin{aligned}\|e_v\|_{L^2(\Gamma_h^0)}&=\|\partial_t e_X\|_{L^2(\Gamma_h^0)}\le\|\partial_t(P_n^*e_X)\|_{L^2(\Gamma_h^0)}+\|\partial_t(P_{\tan}^*e_X)\|_{L^2(\Gamma_h^0)}\\&\lesssim h^{-1}\big(\|\nabla_{\Gamma_h^0}P_{\tan}^*e_X\|_{L^2(\Gamma_h^0)}+\|e_X\|_{L^2(\Gamma_h^0)}\big)+\|d_\kappa\|_{L^2(\Gamma_h^0)}+\|d_v\|_{L^2(\Gamma_h^0)}+h^k.\end{aligned} \tag{4.15}$$

Remark 4 (Existence and uniqueness of finite element solutions)**.** For any given X_h satisfying $\|X_h-X_h^*\|_{L^2(\Gamma_h^0)}\le h^{k-0.1}$ as assumed in (4.4), both $\Gamma_h(t)$ and $\tilde n_h(X_h)$ are also determined. Then (2.2b)–(2.2c) can be viewed as an inhomogeneous linear system governing (v_h,κ_h). This inhomogeneous linear system uniquely determines (v_h,κ_h). To see this, we consider the corresponding homogeneous linear system of $(\hat v_h,\hat\kappa_h)$:

$$\int_{\Gamma_h^0}\hat v_h\cdot[\tilde n_h\circ X_h]\,\chi_n=0, \qquad \forall\,\chi_n\in S_h(\Gamma_h^0), \tag{4.16a}$$

$$\int_{\Gamma_h^0}\hat v_h\cdot\chi_\kappa=\int_{\Gamma_h^0}\hat\kappa_h\,[\tilde n_h\circ X_h]\cdot\chi_\kappa, \qquad \forall\,\chi_\kappa\in S_h(\Gamma_h^0)^3. \tag{4.16b}$$

We show that this homogeneous linear system admits only the trivial solution $(\hat v_h,\hat\kappa_h)=(0,0)$, thereby establishing the existence and uniqueness of solutions (v_h,κ_h) for the inhomogeneous linear system in (2.2b)–(2.2c).

In fact, by choosing $\chi_n=\hat\kappa_h$ in (4.16a) and $\chi_\kappa=\hat v_h$ in (4.16b), we immediately obtain $\hat v_h=0$. Moreover, by choosing $\chi_\kappa=I_h(\hat\kappa_h[n_h^*\circ X_h^*])$ and utilizing the closeness between $\tilde n_h\circ X_h$ and $n_h^*\circ X_h^*$ as shown in Lemma 4.1 (where $e_n:=\tilde n_h\circ X_h-n_h^*\circ X_h^*$), we can derive that $\hat\kappa_h=0$ when h is sufficiently small (the details are omitted here). This would show that the homogeneous linear system in (4.16) admits only the trivial solution. Hence, for any given X_h in the $h^{k-0.1}$-neighborhood of X_h^* in $L^2(\Gamma_h^0)$, the system in (2.2b)–(2.2c) uniquely determines (v_h,κ_h) as a function of X_h.

Moreover, under the condition $\|X_h-X_h^*\|_{L^2(\Gamma_h^0)}\le h^{k-0.1}$ as assumed in (4.4) (i.e., for any X_h in the $h^{k-0.1}$-neighborhood of X_h^* in $L^2(\Gamma_h^0)$), following the proofs of Lemma 4.2 and Lemma 4.5, we can see that if X_h is perturbed by a quantity δ in the L^2 norm (of course, with $\delta\le 2h^{k-0.1}$) then v_h is perturbed by $Ch^{-2}\delta$ in the L^2 norm (in such stability estimates we do not have the terms d_κ, d_v and h^k). Therefore, the function v_h determined by (2.2b)–(2.2c) is locally Lipschitz continuous with respect to X_h. Therefore, according to the local well-posedness of ODE problems, the ODE in (2.2a), with v_h being a locally Lipschitz continuous function of X_h, has a unique solution for $t\in[t_*,t_*+\varepsilon_h]$ for some small $\varepsilon_h>0$. This extends the finite element solutions X_h, v_h and κ_h outside of the time interval $[0,t_*]$.

4.3. Stability estimates

We are now ready to establish the stability estimates for $P_{\tan}^*e_X$ and $e_X\cdot(n_h^*\circ X_h^*)$, which will be used to prove the error estimate in Theorem 2.1.

Proposition 4.1 (Stability estimate for $P_{\tan}^*e_X$)**.** *Under the conditions of Theorem 2.1, there exists a constant $h_0>0$ such that the following stability result holds for $0<h\le h_0$ and $t\in[0,t^*]$:*

$$\begin{aligned}&\frac{\mathrm d}{\mathrm dt}\|P_{\tan}^*e_X\|_{L^2(\Gamma_h^0)}^2+\|\nabla_{\Gamma_h^0}P_{\tan}^*e_X\|_{L^2(\Gamma_h^0)}^2\\&\lesssim\|e_X\|_{L^2(\Gamma_h^0)}^2+h^4\|d_v\|_{L^2(\Gamma_h^0)}^2+h^2\|d_\kappa\|_{L^2(\Gamma_h^0)}^2+\|d_\kappa\|_{H_h^{-1}(\Gamma_h^0)}^2+h^{2k}.\end{aligned} \tag{4.17}$$

Proof. Testing the error equation (4.3c) with $\chi_\kappa=I_hP_{\tan}^*e_X$, we obtain

$$\begin{aligned}&\int_{\Gamma_h^0}\partial_t e_X\cdot I_hP_{\tan}^*e_X+\int_{\Gamma_h^0}\nabla_{\Gamma_h^0}e_X\cdot\nabla_{\Gamma_h^0}I_hP_{\tan}^*e_X\\&=\int_{\Gamma_h^0}\big[\kappa_h(\tilde n_h\circ X_h)-\kappa_h^*(n_h^*\circ X_h^*)\big]\cdot I_hP_{\tan}^*e_X+\int_{\Gamma_h^0}d_\kappa\cdot I_hP_{\tan}^*e_X=:I_1+I_2.\end{aligned} \tag{4.18}$$

The second term on the left-hand side can be decomposed to an approximately tangential component and a remainder term, i.e.,

$$\int_{\Gamma_h^0} \nabla_{\Gamma_h^0} e_X \nabla_{\Gamma_h^0} I_h P_{\tan}^* e_X = \int_{\Gamma_h^0} |\nabla_{\Gamma_h^0} P_{\tan}^* e_X|^2 + \int_{\Gamma_h^0} \nabla_{\Gamma_h^0} P_{\tan}^* e_X \nabla_{\Gamma_h^0} (I_h P_{\tan}^* e_X - P_{\tan}^* e_X)$$
$$+ \int_{\Gamma_h^0} \nabla_{\Gamma_h^0} P_n^* e_X \nabla_{\Gamma_h^0} I_h P_{\tan}^* e_X =: S_1 + S_2 + S_3,$$

where S_2 can be estimated by utilizing the super-approximation property in Lemma 3.7, i.e.,

$$|S_2| \lesssim \|\nabla_{\Gamma_h^0} P_{\tan}^* e_X\|_{L^2(\Gamma_h^0)} h \|e_X\|_{H^1(\Gamma_h^0)} \le C\|e_X\|^2_{L^2(\Gamma_h^0)} + \frac{1}{16}\|\nabla_{\Gamma_h^0} P_{\tan}^* e_X\|^2_{L^2(\Gamma_h^0)}.$$

Moreover, S_3 can be estimated by using (3.17) in Lemma 3.8 (cancellation structure), i.e.,

$$|S_3| \lesssim \|e_X\|_{L^2(\Gamma_h^0)} \big(\|e_X\|_{L^2(\Gamma_h^0)} + \|\nabla_{\Gamma_h^0} P_{\tan}^* e_X\|_{L^2(\Gamma_h^0)}\big)$$
$$\le C\|e_X\|^2_{L^2(\Gamma_h^0)} + \frac{1}{16}\|\nabla_{\Gamma_h^0} P_{\tan}^* e_X\|^2_{L^2(\Gamma_h^0)}.$$

The first term on the left-hand side of (4.18) can be rewrite as follows:

$$\int_{\Gamma_h^0} \partial_t e_X \cdot I_h P_{\tan}^* e_X = \int_{\Gamma_h^0} \partial_t P_n^* e_X \cdot I_h P_{\tan}^* e_X + \int_{\Gamma_h^0} \partial_t P_{\tan}^* e_X \cdot I_h P_{\tan}^* e_X =: J_1 + J_2,$$

where J_1 can be estimated by using (3.18) in Lemma 3.8 (cancellation structure) and (4.15) in Remark 3 (an improved estimate of e_v), i.e.,

$$|J_1| \lesssim \|e_X\|^2_{L^2(\Gamma_h^0)} + h^2\|\partial_t e_X\|_{L^2(\Gamma_h^0)} \big(\|e_X\|_{L^2(\Gamma_h^0)} + \|\nabla_{\Gamma_h^0} P_{\tan}^* e_X\|_{L^2(\Gamma_h^0)}\big)$$
$$\le C\big(\|e_X\|^2_{L^2(\Gamma_h^0)} + h^4\|\partial_t e_X\|^2_{L^2(\Gamma_h^0)}\big) + \frac{1}{16}\|\nabla_{\Gamma_h^0} P_{\tan}^* e_X\|^2_{L^2(\Gamma_h^0)}$$
$$\le C\big(\|e_X\|^2_{L^2(\Gamma_h^0)} + h^4\|d_\kappa\|^2_{L^2(\Gamma_h^0)} + h^4\|d_v\|^2_{L^2(\Gamma_h^0)} + h^{4+2k}\big) + (Ch^2 + \frac{1}{16})\|\nabla_{\Gamma_h^0} P_{\tan}^* e_X\|^2_{L^2(\Gamma_h^0)}.$$

Furthermore, J_2 can be rewritten as follows:

$$J_2 = \int_{\Gamma_h^0} \partial_t P_{\tan}^* e_X \cdot P_{\tan}^* e_X + \int_{\Gamma_h^0} \partial_t P_{\tan}^* e_X \cdot (I_h P_{\tan}^* e_X - P_{\tan}^* e_X)$$
$$=: \frac{1}{2}\frac{\mathrm{d}}{\mathrm{d}t}\int_{\Gamma_h^0} |P_{\tan}^* e_X|^2 + J_3,$$

where J_3 can be estimated with the super-approximation properties in Lemma 3.7, i.e.,

$$|J_3| \lesssim h\|e_X\|_{L^2(\Gamma_h^0)} \|\partial_t P_{\tan}^* e_X\|_{L^2(\Gamma_h^0)}.$$

Then, using (4.13) in Remark 3 (an improved estimate of e_v), we have

$$|J_3| \le C\big(\|e_X\|^2_{L^2(\Gamma_h^0)} + h^2\|d_\kappa\|^2_{L^2(\Gamma_h^0)} + h^4\|d_v\|^2_{L^2(\Gamma_h^0)} + h^{2+2k}\big) + \frac{1}{16}\|\nabla_{\Gamma_h^0} P_{\tan}^* e_X\|^2_{L^2(\Gamma_h^0)}.$$

Therefore, substituting the above estimates into (4.18), we have

$$\begin{aligned} &\frac{1}{2}\frac{\mathrm{d}}{\mathrm{d}t}\|P_{\tan}^* e_X\|^2_{L^2(\Gamma_h^0)} + \frac{5}{8}\|\nabla_{\Gamma_h^0} P_{\tan}^* e_X\|^2_{L^2(\Gamma_h^0)} \\ &\le C\big(\|e_X\|^2_{L^2(\Gamma_h^0)} + h^4\|d_v\|^2_{L^2(\Gamma_h^0)} + h^2\|d_\kappa\|^2_{L^2(\Gamma_h^0)} + h^{2k+2}\big) + |I_1| + |I_2|. \end{aligned} \tag{4.19}$$

It remains to estimate I_1 and I_2, which are defined in (4.18). To this end, we rewrite I_1 into the following several parts:

$$I_1 = \int_{\Gamma_h^0} e_\kappa (n_h^* \circ X_h^*) \cdot I_h P_{\tan}^* e_X + \int_{\Gamma_h^0} \kappa_h^* (\tilde{n}_h^* \circ X_h^* - n_h^* \circ X_h^*) \cdot I_h P_{\tan}^* e_X$$
$$+ \int_{\Gamma_h^0} \kappa_h^* (\tilde{n}_h \circ X_h - \tilde{n}_h^* \circ X_h^*) \cdot I_h P_{\tan}^* e_X + \int_{\Gamma_h^0} e_\kappa e_n \cdot I_h P_{\tan}^* e_X$$
$$=: T_1 + T_2 + T_3 + T_4.$$

Since $I_hP^*_{\tan}e_X = I_hP^*_{\tan}I_hP^*_{\tan}e_X$, it follows that (using the definition $P^*_{\tan} = I - n^*_h(n^*_h)^\top$ and the super-approximation properties)

$$
\begin{aligned}
|T_1| &\lesssim \Big|\int_{\Gamma_h^0} e_\kappa n^*_h\cdot(I_hP^*_{\tan}I_hP^*_{\tan}e_X - P^*_{\tan}I_hP^*_{\tan}e_X)\Big| + \Big|\int_{\Gamma_h^0} e_\kappa n^*_h\cdot(I - n^*_h(n^*_h)^\top)I_hP^*_{\tan}e_X\Big| \\
&\lesssim \|e_\kappa\|_{L^2(\Gamma_h^0)}h^2\|I_hP^*_{\tan}e_X\|_{H^1(\Gamma_h^0)} + \|1-|n^*_h|^2\|_{L^\infty(\Gamma_h^0)}\|e_\kappa\|_{L^2(\Gamma_h^0)}\|e_X\|_{L^2(\Gamma_h^0)} \\
&\lesssim h^2\|e_\kappa\|_{L^2(\Gamma_h^0)}\big(\|\nabla_{\Gamma_h^0}P^*_{\tan}e_X\|_{L^2(\Gamma_h^0)} + \|e_X\|_{L^2(\Gamma_h^0)}\big) \\
&\le C(h^4\|e_\kappa\|^2_{L^2(\Gamma_h^0)} + \|e_X\|^2_{L^2(\Gamma_h^0)}) + \frac{1}{16}\|\nabla_{\Gamma_h^0}P^*_{\tan}e_X\|^2_{L^2(\Gamma_h^0)},
\end{aligned}
$$

where we abbreviate $n^*_h\circ X^*_h$ as n^*_h. By Lemma 3.4 (approximation properties of n^*_h and $\tilde n^*_h$), we have $|T_2|\lesssim h^k\|e_X\|_{L^2(\Gamma_h^0)}$. If we decompose T_3 into four parts by using the decomposition of $\tilde n_h\circ X_h - \tilde n^*_h\circ X^*_h$ in (3.12) of Lemma 3.5 (characterization of $\tilde n_h - \tilde n^*_h$), denoted by $T_3 = T_{31}+T_{32}+T_{33}+T_{34}$, then

$$
\begin{aligned}
T_{32} &= \int_{\Gamma_h^0}\kappa^*_h\big([(\nabla_{\Gamma^*_h(t)}n^*_h)e^*_X]\circ X^*_h\big)\cdot I_hP^*_{\tan}e_X \lesssim \|e_X\|^2_{L^2(\Gamma_h^0)}, \\
T_{33} &= \int_{\Gamma_h^0}\kappa^*_h\big([(\nabla_{\Gamma^*_h(t)}e^*_X)(n^*_h-\tilde n^*_h)]\circ X^*_h\big)\cdot I_hP^*_{\tan}e_X \lesssim h^k\|e_X\|_{L^2(\Gamma_h^0)}, \\
T_{34} &= \int_{\Gamma_h^0}\kappa^*_h\Big(\int_0^1\Big(\int_0^\theta [2(\nabla_{\Gamma_{h,\alpha}}e^\alpha_X)(\nabla_{\Gamma_{h,\alpha}}e^\alpha_X)\tilde n^\alpha_h]\circ X^\alpha_h\,\mathrm{d}\alpha\Big)\,\mathrm{d}\theta\Big)\cdot I_hP^*_{\tan}e_X \\
&\quad - \int_{\Gamma_h^0}\kappa^*_h\Big(\int_0^1\Big(\int_0^\theta [\tilde n^\alpha_h(\tilde n^\alpha_h)^T(\nabla_{\Gamma_{h,\alpha}}e^\alpha_X)^T(\nabla_{\Gamma_{h,\alpha}}e^\alpha_X)\tilde n^\alpha_h]\circ X^\alpha_h\,\mathrm{d}\alpha\Big)\,\mathrm{d}\theta\Big)\cdot I_hP^*_{\tan}e_X,
\end{aligned}
$$

where $\Gamma_{h,\alpha} = \Gamma_{h,\alpha}(t)$ is the intermediate surface defined in (3.1), $\tilde n^\alpha_h$ is the normal vector of $\Gamma_{h,\alpha}$, and e^α_X is the error function defined on $\Gamma_{h,\alpha}$; see (3.2). We see that

$$
\begin{aligned}
|T_{34}| &\lesssim \|\kappa^*_h\|_{L^\infty(\Gamma_h^0)}\Big(\int_0^1\int_0^\theta \|\nabla_{\Gamma_{h,\alpha}}e^\alpha_X\|_{L^\infty(\Gamma_{h,\alpha})}\|\nabla_{\Gamma_{h,\alpha}}e^\alpha_X\|_{L^2(\Gamma_{h,\alpha})}\,\mathrm{d}\alpha\,\mathrm{d}\theta\Big)\|e_X\|_{L^2(\Gamma_h^0)} \\
&\lesssim \|\kappa^*_h\|_{L^\infty(\Gamma_h^0)}\|\nabla_{\Gamma_h^0}e_X\|_{L^\infty(\Gamma_h^0)}\|\nabla_{\Gamma_h^0}e_X\|_{L^2(\Gamma_h^0)}\|e_X\|_{L^2(\Gamma_h^0)} \\
&\lesssim h^{k-2.1-1}\|e_X\|^2_{L^2(\Gamma_h^0)},
\end{aligned}
$$

where the last inequality follows from the inverse inequalities $\|\nabla_{\Gamma_h^0}e_X\|_{L^\infty(\Gamma_h^0)}\le C\,h^{-2}\|e_X\|_{L^2(\Gamma_h^0)}$ and $\|\nabla_{\Gamma_h^0}e_X\|_{L^2(\Gamma_h^0)}\le C\,h^{-1}\|e_X\|_{L^2(\Gamma_h^0)}$, as well as (4.4). This proves that

$$
|T_{34}|\lesssim \|e_X\|^2_{L^2(\Gamma_h^0)} \quad \text{for } k\ge 4. \tag{4.20}
$$

We estimate T_{31} by applying the chain rule of differentiation in (3.4), which implies that

$$
\begin{aligned}
T_{31} &= -\int_{\Gamma_h^0}\kappa^*_h\big([\nabla_{\Gamma^*_h(t)}(e^*_X\cdot n^*_h)]\circ X^*_h\big)\cdot I_hP^*_{\tan}e_X \\
&= -\int_{\Gamma_h^0}\kappa^*_h[\nabla_{\Gamma_h^0}X^*_h + n_{\Gamma_h^0}(n_{\Gamma^*_h(t)}\circ X^*_h)^\top]^{-1}\nabla_{\Gamma_h^0}[e_X\cdot(n^*_h\circ X^*_h)]\cdot I_hP^*_{\tan}e_X.
\end{aligned}
$$

In view of the discussion in Remark 1, we can approximate the possibly discontinuous matrix $\nabla_{\Gamma_h^0}X^*_h + n_{\Gamma_h^0}(n_{\Gamma^*_h(t)}\circ X^*_h)^\top$ by the continuous matrix $[\nabla_{\Gamma^0}X + n_{\Gamma^0}(n_{\Gamma(t)}\circ X)^\top]^{-l}$ with an error bound of $O(h^k)$. This can be used to estimate T_{31} as follows:

$$
\begin{aligned}
|T_{31}| \le &\Big|\int_{\Gamma_h^0}\kappa^*_h[(\nabla_{\Gamma^0}X)^{-l} + (n_{\Gamma^0}(n_{\Gamma(t)}\circ X)^\top)^{-l}]^{-1}\nabla_{\Gamma_h^0}[e_X\cdot(n^*_h\circ X^*_h)]\cdot I_hP^*_{\tan}e_X\Big| \\
&+ Ch^k\|e_X\|_{W^{1,\infty}(\Gamma_h^0)}\|e_X\|_{L^2(\Gamma_h^0)}.
\end{aligned}
$$

In the first term on the right-hand side of the above inequality, we can transfer the gradient from $e_X\cdot(n^*_h\circ X^*_h)$ to $I_hP^*_{\tan}e_X$ by using (3.6) of Lemma 3.3 (integration by parts on Γ_h^0) with $v = \kappa^*_h[(\nabla_{\Gamma^0}X)^{-l} + (n_{\Gamma^0}(n_{\Gamma(t)}\circ X)^\top)^{-l}]^{-1}I_hP^*_{\tan}e_X$. In this process, we can reduce the edge integrals to surface integrals similarly as (3.7) of Lemma 3.3. This, together with $\|e_X\|_{W^{1,\infty}(\Gamma_h^0)} \lesssim 1$ as shown in (4.5), leads to the following result:

$$
\begin{aligned}
|T_{31}| &\lesssim \|e_X\|_{L^2(\Gamma_h^0)}\big(\|\nabla_{\Gamma_h^0}(I_h P_{\tan}^* e_X)\|_{L^2(\Gamma_h^0)} + \|I_h P_{\tan}^* e_X\|_{L^2(\Gamma_h^0)}\big) + h^k\|e_X\|_{L^2(\Gamma_h^0)} \\
&\le C(\|e_X\|_{L^2(\Gamma_h^0)}^2 + h^{2k}) + \frac{1}{16}\|\nabla_{\Gamma_h^0}(P_{\tan}^* e_X)\|_{L^2(\Gamma_h^0)}^2.
\end{aligned}
$$

In summary, we have proved

$$
|T_3| \le C(\|e_X\|_{L^2(\Gamma_h^0)}^2 + h^{2k}) + \frac{1}{16}\|\nabla_{\Gamma_h^0}(P_{\tan}^* e_X)\|_{L^2(\Gamma_h^0)}^2.
$$

T_4 can be estimated with Hölder's inequality and (4.7). The latter can be used to estimate the bound $\|e_n\|_{L^2(\Gamma_h^0)}$, i.e.,

$$
\begin{aligned}
|T_4| &\le \|e_\kappa\|_{L^3(\Gamma_h^0)}\|e_n\|_{L^2(\Gamma_h^0)}\|I_h P_{\tan}^* e_X\|_{L^6(\Gamma_h^0)} \lesssim h^{k-1.1-\frac{1}{3}}\|e_\kappa\|_{L^2(\Gamma_h^0)}\|I_h P_{\tan}^* e_X\|_{H^1(\Gamma_h^0)} \\
&\lesssim h^{2.5}\|e_\kappa\|_{L^2(\Gamma_h^0)}\|I_h P_{\tan}^* e_X\|_{H^1(\Gamma_h^0)} \quad \text{for } k \ge 4 \\
&\lesssim h^{2.5}\|e_\kappa\|_{L^2(\Gamma_h^0)}\big(\|e_X\|_{L^2(\Gamma_h^0)} + \|\nabla_{\Gamma_h^0} P_{\tan}^* e_X\|_{L^2(\Gamma_h^0)}\big) \quad \text{(super-approximation property)} \\
&\le Ch^5\|e_\kappa\|_{L^2(\Gamma_h^0)}^2 + \frac{1}{16}\big(\|e_X\|_{L^2(\Gamma_h^0)}^2 + \|\nabla_{\Gamma_h^0} P_{\tan}^* e_X\|_{L^2(\Gamma_h^0)}^2\big).
\end{aligned}
$$

In summary, combining the above estimates of T_1, T_2, T_3, T_4 and Lemma 4.5 (estimate of e_κ), we have

$$
I_1 \le C\big(\|e_X\|_{L^2(\Gamma_h^0)}^2 + h^4\|d_v\|_{L^2(\Gamma_h^0)}^2 + h^2\|d_\kappa\|_{L^2(\Gamma_h^0)}^2 + h^{2k}\big) + \frac{3}{16}\|\nabla_{\Gamma_h^0}(P_{\tan}^* e_X)\|_{L^2(\Gamma_h^0)}^2.
$$

Finally, I_2 can be estimated by using the definition of $\|d_\kappa\|_{H_h^{-1}(\Gamma_h^0)}$ norm in (4.2) and the super-approximation properties in Lemma 3.7, i.e.,

$$
\begin{aligned}
I_2 &\le \|d_\kappa\|_{H_h^{-1}(\Gamma_h^0)}\|I_h P_{\tan}^* e_X\|_{H^1(\Gamma_h^0)} \\
&\le C\|d_\kappa\|_{H_h^{-1}(\Gamma_h^0)}^2 + \frac{1}{16}\big(\|e_X\|_{L^2(\Gamma_h^0)}^2 + \|\nabla_{\Gamma_h^0} P_{\tan}^* e_X\|_{L^2(\Gamma_h^0)}^2\big).
\end{aligned}
$$

The proof is completed by combining (4.19) with the preceding estimates of $|I_1|$ and $|I_2|$. $\square$

We now turn to analyze the normal component of e_X by considering the error equation in (4.3b), which can be rewritten as follows:

$$
\begin{aligned}
\int_{\Gamma_h^0} \partial_t[e_X \cdot (n_h^* \circ X_h^*)]\chi_n &= \int_{\Gamma_h^0}[u(X_h,t) - u(X_h^*,t)] \cdot (n_h^* \circ X_h^*)\chi_n + \int_{\Gamma_h^0}[u(X_h,t) - v_h^*] \cdot e_n\chi_n \\
&\quad + \int_{\Gamma_h^0} d_v\chi_n + \int_{\Gamma_h^0} e_X \cdot \partial_t(n_h^* \circ X_h^*)\chi_n - \int_{\Gamma_h^0} e_v \cdot e_n\chi_n.
\end{aligned}
\tag{4.21}
$$

The following proposition is proved.

Proposition 4.2 (Stability estimate for $e_X \cdot n_h^*$)**.** *Under the conditions of Theorem 2.1, there exists a constant $h_0 > 0$ such that the following stability result holds uniformly for $0 < h \le h_0$ and $t \in [0, t^*]$:*

$$
\begin{aligned}
\frac{\mathrm{d}}{\mathrm{d}t}\|e_X \cdot (n_h^* \circ X_h^*)\|_{L^2(\Gamma_h^0)}^2 &\le C\big(\|e_X\|_{L^2(\Gamma_h^0)}^2 + \|d_v\|_{L^2(\Gamma_h^0)}^2 + h^2\|d_\kappa\|_{L^2(\Gamma_h^0)}^2 + h^{2k}\big) \\
&\quad + \frac{1}{16}\|\nabla_{\Gamma_h^0} P_{\tan}^* e_X\|_{L^2(\Gamma_h^0)}^2.
\end{aligned}
\tag{4.22}
$$

Proof. For the simplicity of notation, we abbreviate $n_h^* \circ X_h^*$ as n_h^* here (thus n_h^* is used to denote both n_h^* on $\Gamma_h^*(t)$ and $n_h^* \circ X_h^*$ on Γ_h^0 according to the context).

An estimate of $\|e_X \cdot n_h^*\|_{L^2(\Gamma_h^0)}$ can be obtained by choosing $\chi_n := P_{L^2}(e_X \cdot n_h^*)$ in equation (4.21). This yields the following relation:

$$\begin{aligned}
&\frac{1}{2}\frac{\mathrm{d}}{\mathrm{d}t}\|e_X \cdot n_h^*\|^2_{L^2(\Gamma_h^0)} = \int_{\Gamma_h^0} [u(X_h,t) - u(X_h^*,t)] \cdot n_h^* P_{L^2}(e_X \cdot n_h^*) \\
&\quad + \int_{\Gamma_h^0} [u(X_h,t) - v_h^*] \cdot e_n P_{L^2}(e_X \cdot n_h^*) + \int_{\Gamma_h^0} d_v P_{L^2}(e_X \cdot n_h^*) + \int_{\Gamma_h^0} e_X \cdot (\partial_t n_h^*) P_{L^2}(e_X \cdot n_h^*) \\
&\quad + \int_{\Gamma_h^0} \partial_t (e_X \cdot n_h^*)[e_X \cdot n_h^* - P_{L^2}(e_X \cdot n_h^*)] - \int_{\Gamma_h^0} e_v \cdot e_n P_{L^2}(e_X \cdot n_h^*) \\
&=: B_1 + B_2 + B_3 + B_4 + B_5 + B_6.
\end{aligned} \tag{4.23}$$

Utilizing (4.14) in Remark 3 (an improved estimate of e_v), and the super-approximation properties in Lemma 3.7, the term $|B_5|$ can be estimated as follows:

$$\begin{aligned}
|B_5| &\lesssim (h^{-1}\|e_X\|_{L^2(\Gamma_h^0)} + h\|d_\kappa\|_{L^2(\Gamma_h^0)} + \|d_v\|_{L^2(\Gamma_h^0)} + h^k) h \|e_X\|_{L^2(\Gamma_h^0)} \\
&\lesssim \|e_X\|^2_{L^2(\Gamma_h^0)} + h^4\|d_\kappa\|^2_{L^2(\Gamma_h^0)} + h^2\|d_v\|^2_{L^2(\Gamma_h^0)} + h^{2k+2}.
\end{aligned}$$

Furthermore, $|B_1|$, $|B_3|$ and $|B_4|$ can be estimated as follows:

$$|B_1| \lesssim \|e_X\|^2_{L^2(\Gamma_h^0)}, \quad |B_3| \lesssim \|d_v\|_{L^2(\Gamma_h^0)}\|e_X\|_{L^2(\Gamma_h^0)}, \quad |B_4| \lesssim \|e_X\|^2_{L^2(\Gamma_h^0)}.$$

Inequality (4.4) guarantees that both $u(X_h,t)$ and v_h^* are bounded in the $W^{1,\infty}$ norm. Therefore, using the approximation properties of n_h^* and $\tilde n_h^*$ in Lemma 3.4, we have the following estimate of $|B_2|$:

$$\begin{aligned}
|B_2| &\lesssim \Big| \int_{\Gamma_h^0} (u(X_h,t) - v_h^*) \cdot (\tilde n_h - \tilde n_h^*)(e_X \cdot n_h^*) \Big| + \Big| \int_{\Gamma_h^0} (u(X_h,t) - v_h^*) \cdot (\tilde n_h^* - n_h^*)(e_X \cdot n_h^*) \Big| \\
&\quad + \Big| \int_{\Gamma_h^0} (u(X_h,t) - v_h^*) \cdot e_n (P_{L^2}(e_X \cdot n_h^*) - (e_X \cdot n_h^*)) \Big| \\
&\lesssim |B_2^*| + Ch^k \|e_X\|_{L^2(\Gamma_h^0)} + \|e_n\|_{L^2(\Gamma_h^0)} h \|e_X\|_{L^2(\Gamma_h^0)} \\
&\lesssim |B_2^*| + \|e_X\|^2_{L^2(\Gamma_h^0)} + h^{2k},
\end{aligned}$$

where we have used the approximation properties of n_h^* and $\tilde n_h^*$ in Lemma 3.4 in estimating the second term, and the super-approximation property and Lemma 4.1 in estimating the third term. The first term, B_2^*, needs to be estimated by applying (3.12) in Lemma 3.5 (characterization of $\tilde n_h - \tilde n_h^*$), which allows us to decompose B_2^* into four parts, i.e.,

$$B_2^* = B_{21}^* + B_{22}^* + B_{23}^* + B_{24}^*,$$

with

$$B_{21}^* = -\int_{\Gamma_h^0} (u(X_h,t) - v_h^*)\big([\nabla_{\Gamma_h^*(t)}(e_X^* \cdot n_h^*)] \circ X_h^*\big)(e_X \cdot n_h^*) \tag{4.24}$$

$$B_{22}^* = \int_{\Gamma_h^0} (u(X_h,t) - v_h^*)\big([(\nabla_{\Gamma_h^*(t)} n_h^*) e_X^*] \circ X_h^*\big)(e_X \cdot n_h^*) \lesssim \|e_X\|^2_{L^2(\Gamma_h^0)}$$

$$\begin{aligned}
B_{23}^* &= \int_{\Gamma_h^0} (u(X_h,t) - v_h^*)\big([(\nabla_{\Gamma_h^*(t)} e_X^*)(n_h^* - \tilde n_h^*)] \circ X_h^*\big)(e_X \cdot n_h^*) \lesssim h^k \|e_X\|_{L^2(\Gamma_h^0)} \\
&\qquad (\|e_X^*\|_{W^{1,\infty}(\Gamma_h^*(t))} \lesssim 1 \text{ and } \|n_h^* - \tilde n_h^*\|_{L^\infty(\Gamma_h^0)} \lesssim h^k; \text{ see Lemma 3.4})
\end{aligned} \tag{4.25}$$

$$\begin{aligned}
B_{24}^* &= \int_{\Gamma_h^0} (u(X_h,t) - v_h^*)\Big[\int_0^1 \Big(\int_0^\theta \big[2(\nabla_{\Gamma_{h,\alpha}} e_X^\alpha)(\nabla_{\Gamma_{h,\alpha}} e_X^\alpha)\tilde n_h^\alpha \\
&\qquad - \tilde n_h^\alpha (\tilde n_h^\alpha)^T (\nabla_{\Gamma_{h,\alpha}} e_X^\alpha)^T (\nabla_{\Gamma_{h,\alpha}} e_X^\alpha) \tilde n_h^\alpha\big] \circ X_h^\alpha \,\mathrm{d}\alpha\Big) \mathrm{d}\theta\Big](e_X \cdot n_h^*) \\
&\lesssim \|\nabla_{\Gamma_h^0} e_X\|_{L^\infty(\Gamma_h^0)} \|\nabla_{\Gamma_h^0} e_X\|_{L^2(\Gamma_h^0)} \|e_X\|_{L^2(\Gamma_h^0)} \lesssim h^{k-2.1-1}\|e_X\|^2_{L^2(\Gamma_h^0)}.
\end{aligned} \tag{4.26}$$

We further estimate B_{21}^* by using the chain rule of differentiation in (3.4), which allows us to convert $\nabla_{\Gamma_h^*(t)}(e_X^* \cdot n_h^*)$ to $\nabla_{\Gamma_h^0}(e_X \cdot n_h^*)$ in the expression of B_{21}^*, i.e.,

$$\begin{aligned}B_{21}^* &= -\int_{\Gamma_h^0}(u(X_h,t)-v_h^*)[\nabla_{\Gamma_h^0}X_h^* + n_{\Gamma_h^0}(n_{\Gamma_h^*(t)}\circ X_h^*)^\top]^{-1}\nabla_{\Gamma_h^0}(e_X\cdot n_h^*)(e_X\cdot n_h^*)\\ &= -\int_{\Gamma_h^0}(u(X_h,t)-v_h^*)[\nabla_{\Gamma_h^0}X_h^* + n_{\Gamma_h^0}(n_{\Gamma_h^*(t)}\circ X_h^*)^\top]^{-1}\frac{1}{2}\nabla_{\Gamma_h^0}[(e_X\cdot n_h^*)^2].\end{aligned}$$

The discontinuous matrix $[\nabla_{\Gamma_h^0}X_h^* + n_{\Gamma_h^0}(n_{\Gamma_h^*(t)}\circ X_h^*)^\top]^{-1}$ can be further approximated by the continuous matrix $[(\nabla_{\Gamma^0}X)^{-l} + (n_{\Gamma^0}(n_{\Gamma(t)}\circ X)^\top)^{-l}]^{-1}$ with an error of $O(h^k)$. Therefore, using $\|e_X\|_{W^{1,\infty}(\Gamma_h^0)} \lesssim 1$, we have

$$|B_{21}^*| \le \Big|\int_{\Gamma_h^0}(u(X_h,t)-v_h^*)[(\nabla_{\Gamma^0}X)^{-l} + (n_{\Gamma^0}(n_{\Gamma(t)}\circ X)^\top)^{-l}]^{-1}\frac{1}{2}\nabla_{\Gamma_h^0}[(e_X\cdot n_h^*)^2]\Big| + Ch^k\|e_X\|_{L^2(\Gamma_h^0)}.$$

Similarly as we estimate T_{31} (proof of Proposition 4.1), we can transfer the gradient from $(e_X\cdot n_h^*)^2$ to the other functions by using Lemma 3.3 (integration by parts on Γ_h^0). Then we can obtain the following estimate of B_{21}^* :

$$|B_{21}^*| \lesssim \|e_X\|_{L^2(\Gamma_h^0)}^2 + h^{2k}.$$

Combining the estimates of B_{21}^*, B_{22}^*, B_{23}^* and B_{24}^*, we obtain the following result for $k\ge 4$:

$$|B_2| \lesssim \|e_X\|_{L^2(\Gamma_h^0)}^2 + h^{2k}.$$

Finally, B_6 can be estimated by using Hölder's inequality and (4.7), as well as the improved estimate of e_v in Remark 3, i.e.,

$$\begin{aligned}|B_6| &\lesssim \|e_n\|_{L^\infty(\Gamma_h^0)}\|e_v\|_{L^2(\Gamma_h^0)}\|e_X\|_{L^2(\Gamma_h^0)} \lesssim h^{k-2.1}\|e_v\|_{L^2(\Gamma_h^0)}\|e_X\|_{L^2(\Gamma_h^0)}\\ &\lesssim \big(\|\nabla_{\Gamma_h^0}P_{\tan}^*e_X\|_{L^2(\Gamma_h^0)} + \|e_X\|_{L^2(\Gamma_h^0)} + h\|d_\kappa\|_{L^2(\Gamma_h^0)} + h\|d_v\|_{L^2(\Gamma_h^0)} + h^{k+1}\big)\|e_X\|_{L^2(\Gamma_h^0)}\\ &\le C\big(\|e_X\|_{L^2(\Gamma_h^0)}^2 + h^2\|d_\kappa\|_{L^2(\Gamma_h^0)}^2 + h^2\|d_v\|_{L^2(\Gamma_h^0)}^2 + h^{2k+2}\big) + \frac{1}{16}\|\nabla_{\Gamma_h^0}P_{\tan}^*e_X\|_{L^2(\Gamma_h^0)}^2,\end{aligned} \tag{4.27}$$

where the second to last inequality requires $k\ge 4$.

The proof of Proposition 4.2 is completed by combining the estimates of $B_1,\cdots,B_6$. □

5. Error estimates

In this section, we prove Theorem 2.1 by combining Proposition 4.1 (stability estimate for $P_{\tan}^*e_X$), Proposition 4.2 (stability estimate for $e_X\cdot n_h^*$), and estimates of the defects introduced in (4.1). The latter is presented in the following lemma (we refer to Appendix D for more details).

Lemma 5.1 (Estimates of the defects)**.** *Under the conditions of Theorem 2.1, there exists $h_0>0$ such that for all $0<h\le h_0$ and $t\in[0,T]$, the defects d_v and d_κ are bounded as follows*:

$$\|d_v\|_{L^2(\Gamma_h^0)} \lesssim h^k, \quad \|d_\kappa\|_{H_h^{-1}(\Gamma_h^0)} \lesssim h^k \quad \text{and} \quad \|d_\kappa\|_{L^2(\Gamma_h^0)} \lesssim h^{k-1}. \tag{5.1}$$

We are now in a position to prove Theorem 2.1.

Proof of Theorem 2.1. According to Proposition 4.1 (stability estimate for $P_{\tan}^*e_X$), Proposition 4.2 (stability estimate for $e_X\cdot n_h^*$) and Lemma 5.1 (consistency estimate), there exists $h_0>0$ such that for $h\le h_0$ and $t\in[0,t^*]$ the following inequality holds:

$$\begin{aligned}\frac{\mathrm{d}}{\mathrm{d}t}\big(\|P_{\tan}^*e_X\|_{L^2(\Gamma_h^0)}^2 + \|e_X\cdot n_h^*\|_{L^2(\Gamma_h^0)}^2\big) &\lesssim \|e_X\|_{L^2(\Gamma_h^0)}^2 + h^{2k}\\ &\lesssim \big(\|P_{\tan}^*e_X\|_{L^2(\Gamma_h^0)}^2 + \|e_X\cdot n_h^*\|_{L^2(\Gamma_h^0)}^2\big) + h^{2k},\end{aligned}$$

where the last inequality follows from the following equivalence of norms:

$$\|e_X\|^2_{L^2(\Gamma^0_h)} \sim \|P^*_{\tan} e_X\|^2_{L^2(\Gamma^0_h)} + \|P^*_n e_X\|^2_{L^2(\Gamma^0_h)} \sim \|P^*_{\tan} e_X\|^2_{L^2(\Gamma^0_h)} + \|e_X \cdot n^*_h\|^2_{L^2(\Gamma^0_h)},$$

which can be proved similarly as (4.12). By Grönwall's inequality, we obtain

$$\|e_X\|_{L^2(\Gamma^0_h)} \sim \|P^*_{\tan} e_X\|_{L^2(\Gamma^0_h)} + \|e_X \cdot n^*_h\|_{L^2(\Gamma^0_h)} \lesssim h^k. \tag{5.2}$$

By the continuity of the spatially semidiscrete finite element solution in time (which is essentially the solution of an ODE problem as shown in Remark 4), the above estimate implies that (4.4) still holds in a bigger interval $[0, t^* + \varepsilon_h]$ for some $\varepsilon_h > 0$. This proves that $t_* = T$ (otherwise t_* is not maximal, contradicting the assumption at the beginning of Section 4.2). The errors $(X_h)^l - X$ can be decomposed into $(X_h)^l - X = (X_h)^l - (X^*_h)^l + (X^*_h)^l - X$. Then, utilizing inequality (5.2) and the estimates of interpolation error, we have

$$\sup_{t\in[0,T]} \|(X_h)^l - X\|_{L^2(\Gamma^0)} \lesssim \sup_{t\in[0,T]} \|e_X\|_{L^2(\Gamma^0_h)} + \sup_{t\in[0,T]} \|(X^*_h)^l - X\|_{L^2(\Gamma^0)} \lesssim h^k.$$

Moreover, integrating (4.17) from $t = 0$ to $t = T$, we obtain

$$\int_0^T \|(\nabla_{\Gamma^0_h} P^*_{\tan} e_X)^l\|^2_{L^2(\Gamma^0)} \mathrm{d}t \sim \int_0^T \|\nabla_{\Gamma^0_h} P^*_{\tan} e_X\|^2_{L^2(\Gamma^0_h)} \mathrm{d}t \lesssim h^{2k}.$$

Combining [17, Proposition 2.3] and [20, Remark 4.1], we have

$$\|\nabla_{\Gamma^0}(P^*_{\tan})^l - (\nabla_{\Gamma^0_h} P^*_{\tan})^l\|_{L^2(\Gamma^0)} \lesssim h^k, \quad \|\nabla_{\Gamma^0}(e_X)^l - (\nabla_{\Gamma^0_h} e_X)^l\|_{L^2(\Gamma^0)} \lesssim h^k.$$

Then, based on the error estimate between n and its interpolation n^*_h and the preceding estimates, we have

$$\begin{aligned}
\|\nabla_{\Gamma^0}(P_{\tan}(e_X)^l) - (\nabla_{\Gamma^0_h} P^*_{\tan} e_X)^l\|_{L^2(\Gamma^0)} &\le \|\nabla_{\Gamma^0}(P_{\tan}(e_X)^l) - \nabla_{\Gamma^0}((P^*_{\tan})^l (e_X)^l)\|_{L^2(\Gamma^0)} \\
&\quad + \|(\nabla_{\Gamma^0}(P^*_{\tan})^l)(e_X)^l - (\nabla_{\Gamma^0_h} P^*_{\tan})^l (e_X)^l\|_{L^2(\Gamma^0)} \\
&\quad + \|(\nabla_{\Gamma^0}(e_X)^l)(P^*_{\tan})^l - (\nabla_{\Gamma^0_h} e_X)^l (P^*_{\tan})^l\|_{L^2(\Gamma^0)} \lesssim h^k.
\end{aligned}$$

Therefore, combing the estimates above, we have

$$\begin{aligned}
&\int_0^T \|\nabla_{\Gamma^0}(P_{\tan}((X_h)^l - X))\|^2_{L^2(\Gamma^0)} \mathrm{d}t \\
&\lesssim \int_0^T \|\nabla_{\Gamma^0}(P_{\tan}((X^*_h)^l - X))\|^2_{L^2(\Gamma^0)} \mathrm{d}t + \int_0^T \|\nabla_{\Gamma^0}(P_{\tan}(e_X)^l)\|^2_{L^2(\Gamma^0)} \mathrm{d}t \\
&\lesssim \int_0^T \|\nabla_{\Gamma^0}(P_{\tan}((X^*_h)^l - X))\|^2_{L^2(\Gamma^0)} \mathrm{d}t + \int_0^T \|(\nabla_{\Gamma^0_h} P^*_{\tan} e_X)^l\|^2_{L^2(\Gamma^0)} \mathrm{d}t + h^{2k} \lesssim h^{2k}.
\end{aligned}$$

This completes the proof of Theorem 2.1. □

6. Numerical examples

In this section, we present numerical experiments to illustrate the convergence of the proposed method based on the relaxed minimal deformation (RMD) formulation in (1.5), as well as the improvement of mesh quality by the proposed method in comparison with the the surface mesh by the original velocity and the tangential motion with minimal deformation rate (MDR) [1]. In all the numerical examples, a 4-step linearly semi-implicit backward differentiation formula (BDF) is used for time discretization, with a sufficiently small stepsize to guarantee that the errors from time discretization is negligibly small compared with the errors from spatial discretization. At every time level, only a linear system of v_h and κ_h is solved, with X_h being expressed in terms of v_h using the BDF method for (2.2a).

Example 6.1 (Convergence rates)**.** The errors and convergence rates of the proposed method are tested on the evolution of a hypersurface $\Gamma(t) \subset \mathbb{R}^d$ (with $d = 2, 3$) under the following velocity field:

$$u(x) = \begin{cases} (1-|x|)x + (1-|x|)(-x_2, x_1), & d=2, \\ (1-|x|)x + (1-|x|)(-x_2, x_1, 0), & d=3, \end{cases}$$

with the initial surface $\Gamma^0 = \{x \in \mathbb{R}^d : |x| = \frac{1}{2}\}$. In this setting, the exact solution of the equation (1.5) has the following explicit expression:

$$X(p,t) = \frac{r(t)}{r(0)} X(p,0), \qquad \text{for } p \in \Gamma^0,$$

where $X(\cdot,0) = \mathrm{id}(\cdot)$ on Γ^0 and $r(t)$ is governed by the differential equation $\mathrm{d}r/\mathrm{d}t = r(1-r)$. This solution, with initial condition $r(0) = 1/2$, can be expressed as $r(t) = 1/(1+e^{-t})$.

We test the errors of the numerical solutions with mesh sizes $h = \frac{1}{8}, \frac{1}{10}, \frac{1}{12}, \frac{1}{14}, \frac{1}{18}, \frac{1}{20}$, using a 4-step BDF for time discretization with a sufficiently small stepsize $\tau = 2^{-8}$ such that the time discretization errors are negligibly small compared with the spatial discretization errors.

The errors of the numerical solutions are measured in the discrete $L^\infty(0,T;L^2)$ norm of e_X plus the discrete $L^2(0,T;H^1)$ semi-norm norm of $P^*_{\tan} e_X$, with $T = 1/4$, in order to be consistent with the norm used in Theorem 2.1. The numerical results in Figure 1 show that the errors of the numerical solutions are $O(h^k)$ for finite elements of degree $k = 4, 5, 6$. This is consistent with the error estimate proved in Theorem 2.1.

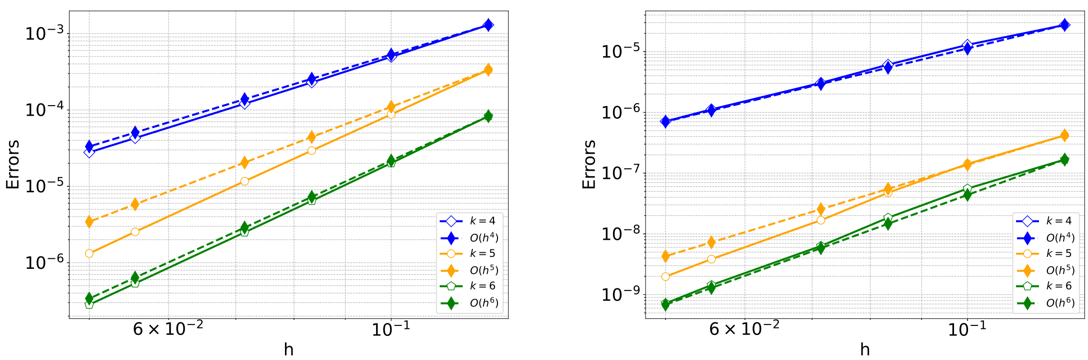

(a) 1D curve (the case $d = 2$) (b) 2D surface (the case $d = 3$)

FIGURE 1. Errors and convergence rates (Example 6.1)

Example 6.2. (Improvement of mesh quality for curve evolution) In this example, we consider the evolution of a 1D curve under the following velocity field:

$$u(x) = x(1-|x|^2) + (1 - 1.2\frac{x_2}{|x|})(-x_2, x_1), \quad x \in \mathbb{R}^2, \tag{6.1}$$

which is shown in Figure 2 (a). The initial curve is an ellipse, given by

$$\Gamma^0 = \{x \in \mathbb{R}^2 : (x_1)^2 + 9(x_2)^2 = 1\}.$$

We compare the evolution of the curve computed by several different methods, including the direct method with the original velocity, the MDR method in [1], and the proposed RMD method in the current paper, using finite elements of degree $k = 4$ and a linearly semi-implicit 4-step BDF time discretization with a time step size of $\tau = 0.001$. The trajectories of the mesh points determined by the original velocity field u, the MDR method in [1], and the RMD method are presented in Figure 2, respectively. It can be observed that the mesh points moving according to the original velocity in (6.1) and the MDR tangential motion both cluster in the upper right corner (either significantly or slightly), while the proposed RMD tangential motion in this paper distribute the mesh points more uniformly, leading to better mesh quality.

Example 6.3. (Improvement of mesh quality for surface evolution) We illustrate the improvement of mesh quality by the RMD method for surfaces which evolve under the velocity

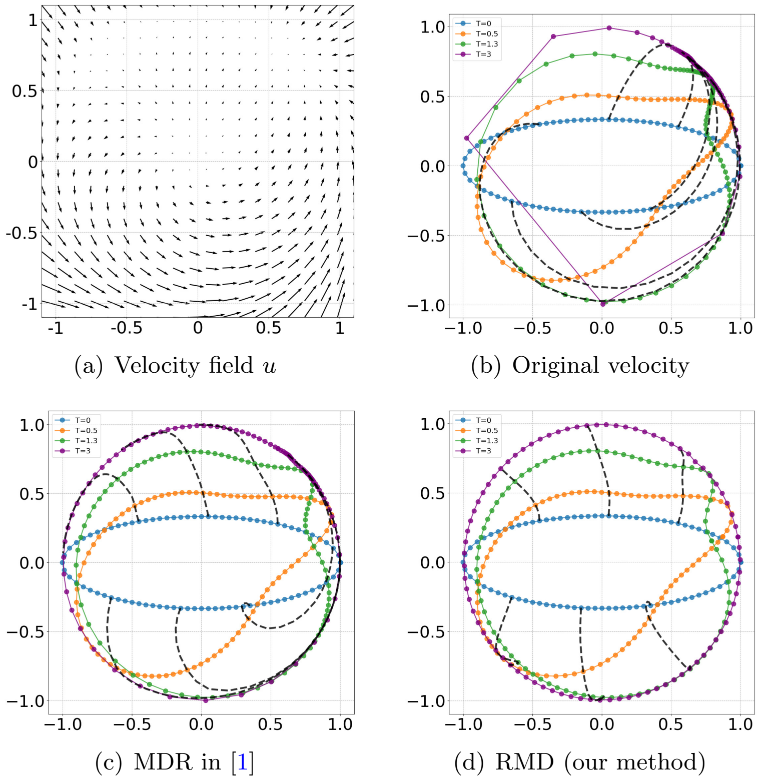

(a) Velocity field u (b) Original velocity

(c) MDR in [1] (d) RMD (our method)

FIGURE 2. Evolution of a curve under velocity (6.1).

field

$$u(x) = x(1 - |x|), \quad x \in \mathbb{R}^3. \tag{6.2}$$

The numerical tests are done by using finite elements of degree $k = 4$. We measure the mesh quality of a surface Γ_h by

$$\sigma_{\max} = \max_{K \subset \Gamma_h} \frac{h(K)}{r(K)},$$

where $h(K)$ represents the diameter of the circumcircle, and $r(K)$ denotes the diameter of the largest inscribed circle for $K \subset \Gamma_h$, respectively.

In the first example, we consider a smooth cell-shape surface given by the following parametrization:

$$\Gamma^0 = \begin{pmatrix} (1 - 0.7(\cos(\varphi)^2 - 1)^2)\sin(\varphi), \\ 2\cos(\varphi)\cos(\theta) \\ 2\cos(\varphi)\sin(\theta) \end{pmatrix}, \quad \theta \in [0, 2\pi) \quad \varphi \in [-\frac{\pi}{2}, \frac{\pi}{2}].$$

In this example, we divide the initial surface into 1678 triangles and utilize the linearly semi-implicit 4-step BDF time discretization with a time step size of $\tau = 0.01$. The surface meshes at different time steps are presented in Figure 3. The mesh qualities are shown in Figure 4, where we compare the RMD method with $k = 4$, the MDR method with $k = 4$, and the lower-order RMD method with $k = 1$. Both results demonstrate that the MDR and RMD tangential motions significantly improve the quality of the surface mesh in this smooth case.

In the second example, we consider a nonsmooth rectangular surface centered at the point $(1/8, 1/8, 1/8)$ with edge lengths of $5/16$, $5/16$, and $30/16$. In this example, we triangulate the initial surface into 6500 triangles and employ the linearly semi-implicit 4-step BDF time discretization with a time step of $\tau = 0.001$. The velocity field in (6.2) exhibits large variation on this initial surface, and the surface undergoes large deformation in the evolution. As a result, the evolution equations for the normal vector and the Weingarten matrix in the MDR method [1] resulted in large errors which make the computation break down at $t = 1.47$. In contrast, our algorithm based on the RMD formulation is stable in the whole process. The surface meshes at different time steps and the mesh qualities are presented in Figures 5 and 6, where the numerical result obtained using the MDR method is not displayed due to the breakdown of computation, while the proposed RMD method in this paper still produces a good shape of triangles with significantly improved mesh quality.

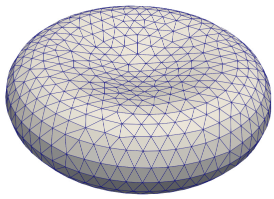

(a) Initial surface

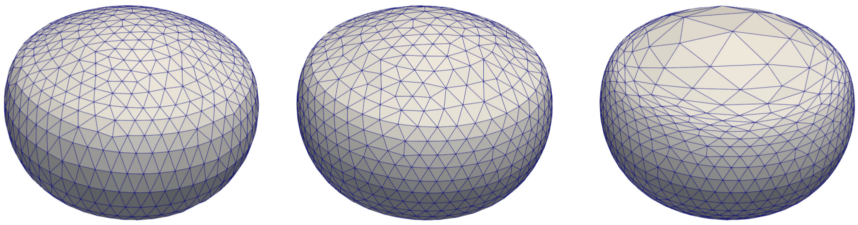

(b) MDR in [1], $t = 2$ (c) RMD (our method), $t = 2$ (d) Original velocity, $t = 2$

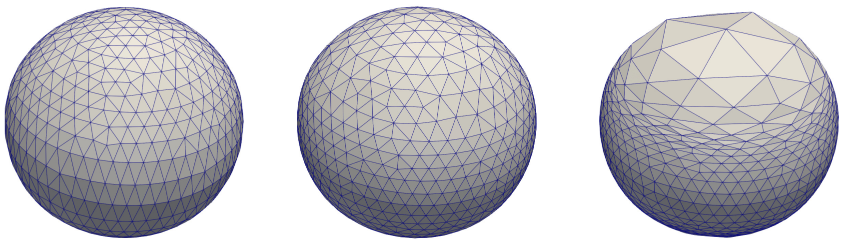

(e) MDR in [1], $t = 4$ (f) RMD (our method), $t = 4$ (g) Original velocity, $t = 4$

FIGURE 3. Evolution of surface under velocity (6.2) (smooth initial surface).

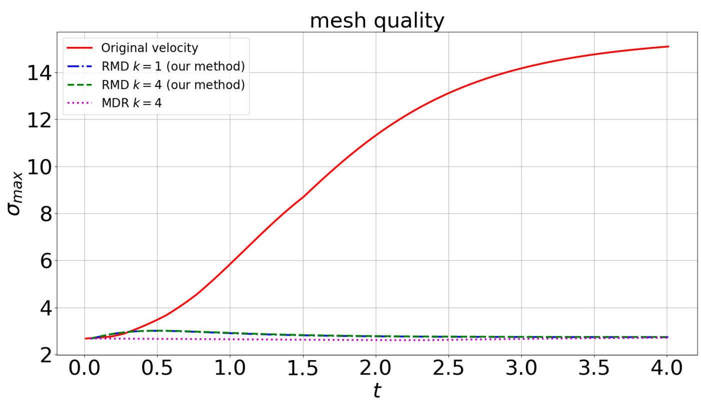

FIGURE 4. Mesh quality of surface under velocity (6.2) (smooth initial surface).

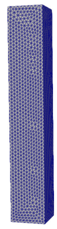

(a) Initial surface

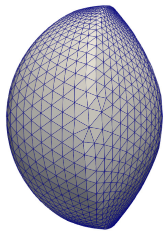

(b) RMD (our method), $t = 3.3$

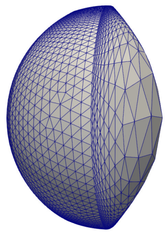

(c) Original velocity, $t = 3.3$

(d) MDR in [1] (computation breaks down)

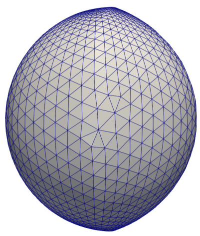

(e) RMD (our method), $t = 4.5$

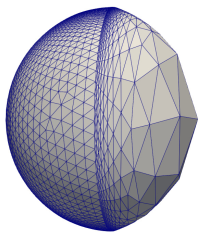

(f) Original velocity, $t = 4.5$

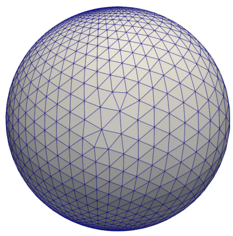

(g) RMD (our method), $t = 10$

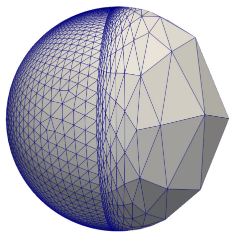

(h) Original velocity, $t = 10$

FIGURE 5. Evolution of surface under velocity (6.2) (nonsmooth initial surface).

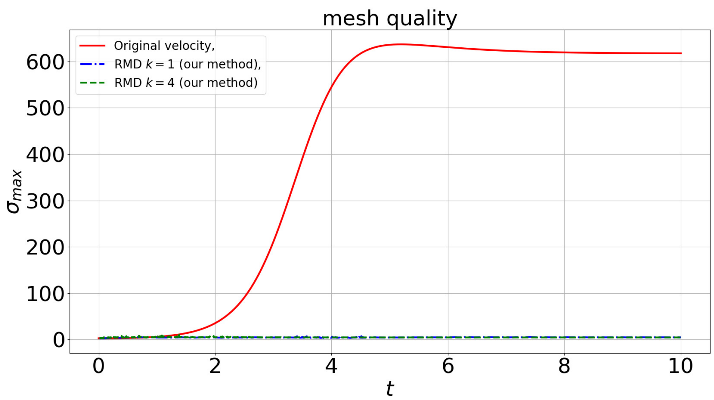

FIGURE 6. Mesh quality of surface under velocity (6.2) (nonsmooth initial surface).

7. Conclusion

We have proposed a relaxed minimal deformation (RMD) formulation of surface evolution with a tangential motion generated by harmonic map heat flow from the initial surface Γ^0 onto the evolving surface $\Gamma(t)$. Differently from the MDR formulation studied in [1], the proposed RMD formulation intentionally avoids solving an additional evolution equation of n, which often causes the numerical solution of n to differ from the normal vector of the numerically-solved surface when the surface undergoes large deformation. Numerically, the tangential motion generated by this RMD formulation improves the mesh quality of evolving surfaces as effectively as the MD formulation in (1.4). Theoretically, we have proved convergence of finite element approximations to the RMD formulation of surface evolution with high-order accuracy for finite elements of degree $k \geq 4$ (this cannot be proved for the MD formulation so far). The restriction to finite elements of degree $k \geq 4$ in the convergence proof is used at several places, i.e., (4.20), (4.26) and (4.27), to control some nonlinear terms appearing in the error analysis. Convergence of finite element approximations to the RMD formulation for low-order finite elements of degree $k = 1, 2, 3$, as well as the development of other convergent algorithms which have similar advantages as the RMD formulation and could be proved convergent for low-order finite elements, is an interesting and challenging task.

Acknowledgments

This work was supported in part by the Research Grants Council of the Hong Kong Special Administrative Region, China (Project No. PolyU/RFS2324-5S03, PolyU/GRF15304024), AMSS-PolyU Joint Laboratory, and an internal grant of Hong Kong Polytechnic University (Project ID: P0051154).

References

[1] Genming Bai, Jiashun Hu, and Buyang Li. A convergent evolving finite element method with artificial tangential motion for surface evolution under a prescribed velocity field. *SIAM Journal on Numerical Analysis*, 62(5):2172–2195, 2024.

[2] Genming Bai and Buyang Li. Convergence of a stabilized parametric finite element method of the Barrett-Garcke-Nürnberg type for curve shortening flow. *Mathematics of Computation*, 2025, 70 pages, DOI: https://doi.org/10.1090/mcom/4019.

[3] Eberhard Bänsch. Finite element discretization of the Navier–Stokes equations with a free capillary surface. *Numerische Mathematik*, 88:203–235, 2001.

[4] Eberhard Bänsch, Pedro Morin, and Ricardo H Nochetto. A finite element method for surface diffusion: the parametric case. *Journal of Computational Physics*, 203(1):321–343, 2005.

[5] Weizhu Bao, Harald Garcke, Robert Nürnberg, and Quan Zhao. Volume-preserving parametric finite element methods for axisymmetric geometric evolution equations. *Journal of Computational Physics*, 460:111180, 2022.

[6] Weizhu Bao, Wei Jiang, Yan Wang, and Quan Zhao. A parametric finite element method for solid-state dewetting problems with anisotropic surface energies. *Journal of Computational Physics*, 330:380–400, 2017.

[7] Weizhu Bao and Quan Zhao. An energy-stable parametric finite element method for simulating solid-state dewetting problems in three dimensions. *Journal of Computational Mathematics*, 41(4):771–796, 2023.

[8] John W. Barrett, Harald Garcke, and Robert Nürnberg. A parametric finite element method for fourth order geometric evolution equations. *Journal of Computational Physics*, 222(1):441–467, 2007.

[9] John W. Barrett, Harald Garcke, and Robert Nürnberg. On the parametric finite element approximation of evolving hypersurfaces in $\mathbb{R}^3$. *Journal of Computational Physics*, 227(9):4281–4307, 2008.

[10] John W. Barrett, Harald Garcke, and Robert Nürnberg. Parametric approximation of Willmore flow and related geometric evolution equations. *SIAM Journal on Scientific Computing*, 31(1):225–253, 2008.

[11] John W. Barrett, Harald Garcke, and Robert Nürnberg. Elastic flow with junctions: variational approximation and applications to nonlinear splines. *Mathematical Models and Methods in Applied Sciences*, 22(11):1250037, 2012.

[12] John W. Barrett, Harald Garcke, and Robert Nürnberg. Eliminating spurious velocities with a stable approximation of viscous incompressible two-phase Stokes flow. *Computer Methods in Applied Mechanics and Engineering*, 267:511–530, 2013.

[13] John W. Barrett, Harald Garcke, and Robert Nürnberg. Parametric finite element approximations of curvature-driven interface evolutions. In *Handbook of numerical analysis*, volume 21, pages 275–423. Elsevier, 2020.

[14] Andrea Bonito, Ricardo H. Nochetto, and M Sebastian Pauletti. Parametric FEM for geometric biomembranes. *Journal of Computational Physics*, 229(9):3171–3188, 2010.

[15] Klaus Deckelnick, Gerhard Dziuk, and Charles M. Elliott. Computation of geometric partial differential equations and mean curvature flow. *Acta Numerica*, 14:139–232, 2005.

[16] Klaus Deckelnick and Vanessa Styles. Stability and error analysis for a diffuse interface approach to an advection–diffusion equation on a moving surface. *Numerische Mathematik*, 139:709–741, 2018.
[17] Alan Demlow. Higher-order finite element methods and pointwise error estimates for elliptic problems on surfaces. *SIAM Journal on Numerical Analysis*, 47(2):805–827, 2009.
[18] Beiping Duan and Buyang Li. New artificial tangential motions for parametric finite element approximation of surface evolution. *SIAM Journal on Scientific Computing*, 46(1):A587–A608, 2024.
[19] Gerhard Dziuk. Computational parametric Willmore flow. *Numerische Mathematik*, 111:55–80, 2008.
[20] Gerhard Dziuk and Charles Elliott. L^2-estimates for the evolving surface finite element method. *Mathematics of Computation*, 82(281):1–24, 2013.
[21] Gerhard Dziuk and Charles M. Elliott. Finite elements on evolving surfaces. *IMA Journal of Numerical Analysis*, 27(2):262–292, 2007.
[22] Gerhard Dziuk and Charles M. Elliott. A fully discrete evolving surface finite element method. *SIAM Journal on Numerical Analysis*, 50(5):2677–2694, 2012.
[23] Gerhard Dziuk and Charles M. Elliott. Finite element methods for surface PDEs. *Acta Numerica*, 22:289–396, 2013.
[24] Gerhard Dziuk, Dietmar Kröner, and Thomas Müller. Scalar conservation laws on moving hypersurfaces. *Interfaces and Free Boundaries*, 15(2):203–236, 2013.
[25] Klaus Ecker. *Regularity theory for mean curvature flow*, volume 57. Springer Science & Business Media, 2012.
[26] Charles M. Elliott and Hans Fritz. On algorithms with good mesh properties for problems with moving boundaries based on the harmonic map heat flow and the Deturck trick. *The SMAI Journal of Computational Mathematics*, 2:141–176, 2016.
[27] Charles M. Elliott and Thomas Ranner. Evolving surface finite element method for the Cahn–Hilliard equation. *Numerische Mathematik*, 129(3):483–534, 2015.
[28] Charles M. Elliott and Vanessa Styles. An ALE ESFEM for solving PDEs on evolving surfaces. *Milan Journal of Mathematics*, 80(2):469–501, 2012.
[29] Guosheng Fu. Arbitrary Lagrangian–Eulerian hybridizable discontinuous Galerkin methods for incompressible flow with moving boundaries and interfaces. *Computer Methods in Applied Mechanics and Engineering*, 367:113158, 2020.
[30] Sashikumaar Ganesan, Andreas Hahn, Kristin Simon, and Lutz Tobiska. ALE-FEM for two-phase and free surface flows with surfactants. *Transport Processes at Fluidic Interfaces*, pages 5–31, 2017.
[31] Jiashun Hu and Buyang Li. Evolving finite element methods with an artificial tangential velocity for mean curvature flow and Willmore flow. *Numerische Mathematik*, 152(1):127–181, 2022.
[32] Balázs Kovács, Buyang Li, and Christian Lubich. A convergent evolving finite element algorithm for mean curvature flow of closed surfaces. *Numerische Mathematik*, 143:797–853, 2019.
[33] Balázs Kovács, Buyang Li, and Christian Lubich. A convergent evolving finite element algorithm for Willmore flow of closed surfaces. *Numerische Mathematik*, 149(3):595–643, 2021.
[34] Balázs Kovács, Buyang Li, Christian Lubich, and Christian A Power Guerra. Convergence of finite elements on an evolving surface driven by diffusion on the surface. *Numerische Mathematik*, 137:643–689, 2017.
[35] Balázs Kovács and Christian Andreas Power Guerra. Higher order time discretizations with ALE finite elements for parabolic problems on evolving surfaces. *IMA Journal of Numerical Analysis*, 38(1):460–494, 2018.
[36] Christoph Lehrenfeld, Maxim A Olshanskii, and Xianmin Xu. A stabilized trace finite element method for partial differential equations on evolving surfaces. *SIAM Journal on Numerical Analysis*, 56(3):1643–1672, 2018.
[37] Charles M. Elliott and Hans Fritz. On approximations of the curve shortening flow and of the mean curvature flow based on the Deturck trick. *IMA Journal of Numerical Analysis*, 37(2):543–603, 2017.
[38] Carlo Mantegazza. *Lecture Notes on Mean Curvature Flow*, volume 290. Springer Science & Business Media, 2011.
[39] Emilie Marchandise, C Carton de Wiart, WG Vos, Christophe Geuzaine, and J-F Remacle. High-quality surface remeshing using harmonic maps — Part II: Surfaces with high genus and of large aspect ratio. *International Journal for Numerical Methods in Engineering*, 86(11):1303–1321, 2011.
[40] Alina Mierswa. *Error estimates for a finite difference approximation of mean curvature flow for surfaces of torus type*. PhD thesis, 2020.
[41] J-F Remacle, Christophe Geuzaine, Gaëtan Compere, and Emilie Marchandise. High-quality surface remeshing using harmonic maps. *International Journal for Numerical Methods in Engineering*, 83(4):403–425, 2010.
[42] Thomas Richter. *Fluid-structure Interactions: Models, Analysis and Finite Elements*, volume 118. Springer, 2017.
[43] Jan Steinhilber. *Numerical analysis for harmonic maps between hypersurfaces and grid improvement for computational parametric geometric flows*. PhD thesis, Dissertation, Albert-Ludwigs-Universität Freiburg, 2014, 2014.
[44] Quan Zhao, Wei Jiang, and Weizhu Bao. A parametric finite element method for solid-state dewetting problems in three dimensions. *SIAM Journal on Scientific Computing*, 42(1):B327–B352, 2020.

Appendix. More details in the stability estimates

Appendix A. Proof of Lemma 4.3

Note that $\partial_t(P^*_{\tan}e_X)$ can be well approximated by $\partial_t I_h(P^*_{\tan}e_X)$ with the super-approximation properties in Lemma 3.7, i.e.,

$$\begin{aligned}
&\|\partial_t(P^*_{\tan}e_X) - \partial_t I_h(P^*_{\tan}e_X)\|_{L^2(\Gamma_h^0)} = \|\partial_t(P^*_{\tan}e_X) - I_h\partial_t(P^*_{\tan}e_X)\|_{L^2(\Gamma_h^0)} \\
&\le \|(\partial_t P^*_{\tan})e_X - I_h((\partial_t P^*_{\tan})e_X)\|_{L^2(\Gamma_h^0)} + \|P^*_{\tan}(\partial_t e_X) - I_h(P^*_{\tan}(\partial_t e_X))\|_{L^2(\Gamma_h^0)} \\
&\lesssim h\big(\|e_X\|_{L^2(\Gamma_h^0)} + \|\partial_t e_X\|_{L^2(\Gamma_h^0)}\big).
\end{aligned} \tag{A.1}$$

By using this result and the super-approximation properties in Lemma 3.7 again, we derive the following estimates for any test function $\phi_h \in S_h(\Gamma_h^0)^3$:

$$\begin{aligned}
&\int_{\Gamma_h^0} \partial_t(I_h P^*_{\tan}e_X)\phi_h = \int_{\Gamma_h^0} I_h(\partial_t P^*_{\tan}e_X)\phi_h \\
&\lesssim \int_{\Gamma_h^0} \partial_t(P^*_{\tan}e_X)\phi_h + \|I_h(\partial_t P^*_{\tan}e_X) - \partial_t(P^*_{\tan}e_X)\|_{L^2(\Gamma_h^0)}\|\phi_h\|_{L^2(\Gamma_h^0)} \quad \text{(triangle inequality)} \\
&\lesssim \int_{\Gamma_h^0} (\partial_t e_X)P^*_{\tan}\phi_h + \int_{\Gamma_h^0} (\partial_t P^*_{\tan})e_X\phi_h + h(\|e_X\|_{L^2(\Gamma_h^0)} + \|\partial_t e_X\|_{L^2(\Gamma_h^0)})\|\phi_h\|_{L^2(\Gamma_h^0)} \\
&\lesssim \int_{\Gamma_h^0} \partial_t e_X\big[I_h(P^*_{\tan}\phi_h) + P^*_{\tan}\phi_h - I_h(P^*_{\tan}\phi_h)\big] + (\|e_X\|_{L^2(\Gamma_h^0)} + h\|\partial_t e_X\|_{L^2(\Gamma_h^0)})\|\phi_h\|_{L^2(\Gamma_h^0)} \\
&\lesssim \int_{\Gamma_h^0} \partial_t e_X I_h(P^*_{\tan}\phi_h) + (\|e_X\|_{L^2(\Gamma_h^0)} + h\|\partial_t e_X\|_{L^2(\Gamma_h^0)})\|\phi_h\|_{L^2(\Gamma_h^0)}.
\end{aligned} \tag{A.2}$$

The first term on the right-hand side of (A.2) can be estimated by choosing test function $\chi_\kappa = I_h P^*_{\tan}\phi_h$ in weak formulation (4.3c), i.e.,

$$\begin{aligned}
\int_{\Gamma_h^0} \partial_t e_X I_h P^*_{\tan}\phi_h =& -\int_{\Gamma_h^0} \nabla_{\Gamma_h^0} P^*_{\tan}e_X \nabla_{\Gamma_h^0} I_h P^*_{\tan}\phi_h - \int_{\Gamma_h^0} \nabla_{\Gamma_h^0} P^*_n e_X \nabla_{\Gamma_h^0} I_h P^*_{\tan}\phi_h \\
&+ \int_{\Gamma_h^0} e_\kappa n_h^* \cdot I_h P^*_{\tan}\phi_h + \int_{\Gamma_h^0} \kappa_h^* e_n \cdot I_h P^*_{\tan}\phi_h + \int_{\Gamma_h^0} e_\kappa e_n \cdot I_h P^*_{\tan}\phi_h + \int_{\Gamma_h^0} d_\kappa \cdot I_h P^*_{\tan}\phi_h \\
=:& \, T_1 + T_2 + T_3 + T_4 + T_5 + T_6.
\end{aligned}$$

where T_1 is estimated by converting $\|\nabla_{\Gamma_h^0} I_h P^*_{\tan}\phi_h\|_{L^2(\Gamma_h^0)}$ to $\|\nabla_{\Gamma_h^0} P^*_{\tan}\phi_h\|_{L^2(\Gamma_h^0)} + \|\phi_h\|_{L^2(\Gamma_h^0)}$ using the super-approximation properties in Lemma 3.7:

$$\begin{aligned}
|T_1| &\lesssim \|\nabla_{\Gamma_h^0} P^*_{\tan}e_X\|_{L^2(\Gamma_h^0)}(\|\nabla_{\Gamma_h^0} P^*_{\tan}\phi_h\|_{L^2(\Gamma_h^0)} + \|\phi_h\|_{L^2(\Gamma_h^0)}) \\
&\lesssim h^{-1}\|\nabla_{\Gamma_h^0} P^*_{\tan}e_X\|_{L^2(\Gamma_h^0)}\|\phi_h\|_{L^2(\Gamma_h^0)},
\end{aligned}$$

where the inverse inequality $\|\nabla_{\Gamma_h^0} P^*_{\tan}\phi_h\|_{L^2(\Gamma_h^0)} \le C h^{-1}\|P^*_{\tan}\phi_h\|_{L^2(\Gamma_h^0)} \le C h^{-1}\|\phi_h\|_{L^2(\Gamma_h^0)}$ is used. Similarly, T_3 can be estimated with the following decomposition and the super-approximation properties again:

$$\begin{aligned}
T_3 &= \int_{\Gamma_h^0} e_\kappa n_h^* \cdot (I_h P^*_{\tan}\phi_h - P^*_{\tan}\phi_h) + \int_{\Gamma_h^0} e_\kappa n_h^* \cdot P^*_{\tan}\phi_h \\
&\lesssim h\|e_\kappa\|_{L^2(\Gamma_h^0)}\|\phi_h\|_{L^2(\Gamma_h^0)} + \Big|\int_{\Gamma_h^0} e_\kappa n_h^* \cdot (I_{3\times 3} - n_h^*(n_h^*)^T)\phi_h\Big| \\
&\lesssim \big(h + \|1 - |n_h^*|^2\|_{L^\infty(\Gamma_h^0)}\big)\|e_\kappa\|_{L^2(\Gamma_h^0)}\|\phi_h\|_{L^2(\Gamma_h^0)} \\
&\lesssim h\|e_\kappa\|_{L^2(\Gamma_h^0)}\|\phi_h\|_{L^2(\Gamma_h^0)},
\end{aligned}$$

where the last inequality follows from Lemma 3.4 (approximation properties of n_h^* and $\tilde{n}_h^*$).

Moreover, T_2 can be estimated with the cancellation structure stated in (3.17) of Lemma 3.8, i.e.,

$$|T_2| \lesssim \|e_X\|_{L^2(\Gamma_h^0)}\big(\|\phi_h\|_{L^2(\Gamma_h^0)} + \|\nabla_{\Gamma_h^0}(P^*_{\tan}\phi_h)\|_{L^2(\Gamma_h^0)}\big) \lesssim h^{-1}\|e_X\|_{L^2(\Gamma_h^0)}\|\phi_h\|_{L^2(\Gamma_h^0)}.$$

Additionally, by employing (4.7) and Lemma 4.1 (an estimate of e_n), we can estimate T_4 and T_5 as follows:

$$|T_4| \lesssim \|\kappa_h^*\|_{L^\infty(\Gamma_h^0)}\|e_n\|_{L^2(\Gamma_h^0)}\|\phi_h\|_{L^2(\Gamma_h^0)} \lesssim \big(h^{-1}\|e_X\|_{L^2(\Gamma_h^0)} + h^k\big)\|\phi_h\|_{L^2(\Gamma_h^0)},$$
$$|T_5| \lesssim \|e_n\|_{L^\infty(\Gamma_h^0)}\|e_\kappa\|_{L^2(\Gamma_h^0)}\|\phi_h\|_{L^2(\Gamma_h^0)} \lesssim h\|e_\kappa\|_{L^2(\Gamma_h^0)}\|\phi_h\|_{L^2(\Gamma_h^0)} \quad \text{for} \quad k \geq 4.$$

Finally, we also observe that $|T_6| \lesssim \|d_\kappa\|_{L^2(\Gamma_h^0)}\|\phi_h\|_{L^2(\Gamma_h^0)}$.

Therefore, by choosing $\phi_h = \partial_t(I_h P_{\tan}^* e_X)$ in (A.2), and substituting the estimates for $T_1, \cdots, T_6$ into (A.2), we obtain

$$\begin{aligned}\|\partial_t I_h P_{\tan}^* e_X\|_{L^2(\Gamma_h^0)} \lesssim h\|\partial_t e_X\|_{L^2(\Gamma_h^0)} &+ h^{-1}\big(\|\nabla_{\Gamma_h^0} P_{\tan}^* e_X\|_{L^2(\Gamma_h^0)} + \|e_X\|_{L^2(\Gamma_h^0)}\big)\\ &+ \|d_\kappa\|_{L^2(\Gamma_h^0)} + h\|e_\kappa\|_{L^2(\Gamma_h^0)} + h^k.\end{aligned} \tag{A.3}$$

The left-hand side of (A.3) can be replaced by $\|\partial_t P_{\tan}^* e_X\|_{L^2(\Gamma_h^0)}$ with (A.1), and $h\|\partial_t e_X\|_{L^2(\Gamma_h^0)}$ from Lemma 4.2. This proves Lemma 4.3. □

Appendix B. Proof of Lemma 4.4

Choosing test function $\chi_n := P_{L^2}\partial_t(e_X \cdot n_h^*)$ in weak formulation (4.3b), we obtain the following relation:

$$\begin{aligned}&\int_{\Gamma_h^0} |\partial_t(e_X \cdot n_h^*)|^2 + \int_{\Gamma_h^0} \partial_t(e_X \cdot n_h^*)(P_{L^2}\partial_t(e_X \cdot n_h^*) - \partial_t(e_X \cdot n_h^*))\\
&= \int_{\Gamma_h^0} [u(X_h,t) - u(X_h^*,t)] \cdot n_h^* P_{L^2}(\partial_t(e_X \cdot n_h^*)) + \int_{\Gamma_h^0} (u(X_h) - v_h^*) \cdot e_n P_{L^2}(\partial_t(e_X \cdot n_h^*))\\
&\quad - \int_{\Gamma_h^0} e_v \cdot e_n P_{L^2}(\partial_t(e_X \cdot n_h^*)) + \int_{\Gamma_h^0} (e_X \cdot \partial_t n_h^* - d_v) P_{L^2}(\partial_t(e_X \cdot n_h^*))\\
&=: A_1 + A_2 + A_3 + A_4.\end{aligned} \tag{B.1}$$

The second term on the left-hand side of (B.1) can be estimated with the following result (which follows from the Leibniz rule of differentiation and the super-approximation properties in Lemma 3.7):

$$\begin{aligned}&\|P_{L^2}\partial_t(e_X \cdot n_h^*) - \partial_t(e_X \cdot n_h^*)\|_{L^2(\Gamma_h^0)}\\
&\leq \|P_{L^2}(\partial_t e_X \cdot n_h^*) - \partial_t e_X \cdot n_h^*\|_{L^2(\Gamma_h^0)} + \|P_{L^2}(e_X \cdot \partial_t n_h^*) - e_X \cdot \partial_t n_h^*\|_{L^2(\Gamma_h^0)}\\
&\lesssim h(\|\partial_t e_X\|_{L^2(\Gamma_h^0)} + \|e_X\|_{L^2(\Gamma_h^0)}).\end{aligned}$$

The right-hand side of (B.1) can be estimated by using Lemma 4.1 (an estimate of e_n), smoothness of velocity field u, and (4.7):

$$\begin{aligned}&|A_1| \lesssim \|e_X\|_{L^2(\Gamma_h^0)}\|\partial_t(e_X \cdot n_h^*)\|_{L^2(\Gamma_h^0)},\\
&|A_2| \lesssim \|e_n\|_{L^2(\Gamma_h^0)}\|\partial_t(e_X \cdot n_h^*)\|_{L^2(\Gamma_h^0)} \lesssim (h^{-1}\|e_X\|_{L^2(\Gamma_h^0)} + h^k)\|\partial_t(e_X \cdot n_h^*)\|_{L^2(\Gamma_h^0)},\\
&|A_3| \lesssim \|e_n\|_{L^\infty(\Gamma_h^0)}\|e_v\|_{L^2(\Gamma_h^0)}\|\partial_t(e_X \cdot n_h^*)\|_{L^2(\Gamma_h^0)} \lesssim h\|\partial_t e_X\|_{L^2(\Gamma_h^0)}\|\partial_t(e_X \cdot n_h^*)\|_{L^2(\Gamma_h^0)},\\
&|A_4| \lesssim (\|d_v\|_{L^2(\Gamma_h^0)} + \|e_X\|_{L^2(\Gamma_h^0)})\|\partial_t(e_X \cdot n_h^*)\|_{L^2(\Gamma_h^0)},\end{aligned}$$

where the above estimate of $|A_3|$ requires $k \geq 4$ to guarantee that $\|e_n\|_{L^\infty(\Gamma_h^0)} \lesssim h$.

The term $\|\partial_t e_X\|_{L^2(\Gamma_h^0)}$ in the above inequalities can be estimated by using Lemma 4.2. Then, substituting the estimates of $\|P_{L^2}\partial_t(e_X \cdot n_h^*) - \partial_t(e_X \cdot n_h^*)\|_{L^2(\Gamma_h^0)}$ and $|A_j|$, $j = 1, 2, 3, 4$, into (B.1), we obtain the result of Lemma 4.4. □

Appendix C. Proof of Lemma 4.5

By using estimate (3.10a) in Lemma 3.4 (approximation properties of n_h^* and $\tilde{n}_h^*$) we can derive the following inequality:

$$\big|\|e_\kappa\|_{L^2(\Gamma_h^0)}^2 - \|e_\kappa n_h^*\|_{L^2(\Gamma_h^0)}^2\big| \leq \|e_\kappa\|_{L^2(\Gamma_h^0)}^2 \||n_h^*|^2 - 1\|_{L^\infty(\Gamma_h^0)} \lesssim h^{k+1}\|e_\kappa\|_{L^2(\Gamma_h^0)}^2.$$

For sufficiently small h (smaller than some constant), $h^{k+1}\|e_\kappa\|^2_{L^2(\Gamma_h^0)}$ is much smaller than $\|e_\kappa\|^2_{L^2(\Gamma_h^0)}$. In this case, the last inequality implies the following equivalence of norms:

$$\|e_\kappa\|_{L^2(\Gamma_h^0)} \sim \|e_\kappa n_h^*\|_{L^2(\Gamma_h^0)}. \tag{C.1}$$

By choosing test function $\chi_\kappa := P_{L^2}(e_\kappa n_h^*)$ in weak formulation (4.3c), we obtain the following expression of $\|e_\kappa n_h^*\|_{L^2(\Gamma_h^0)}$:

$$\begin{aligned}\|e_\kappa n_h^*\|^2_{L^2(\Gamma_h^0)} &= \int_{\Gamma_h^0} e_\kappa n_h^* \cdot (e_\kappa n_h^* - P_{L^2}(e_\kappa n_h^*)) - \int_{\Gamma_h^0} \kappa_h^* e_n \cdot P_{L^2}(e_\kappa n_h^*) \\ &\quad - \int_{\Gamma_h^0} e_\kappa e_n \cdot P_{L^2}(e_\kappa n_h^*) - \int_{\Gamma_h^0} d_\kappa \cdot P_{L^2}(e_\kappa n_h^*) + \int_{\Gamma_h^0} \partial_t e_X \cdot P_{L^2}(e_\kappa n_h^*) \\ &\quad + \int_{\Gamma_h^0} \nabla_{\Gamma_h^0} e_X \cdot \nabla_{\Gamma_h^0} P_{L^2}(e_\kappa n_h^*) \\ &=: M_1 + M_2 + M_3 + M_4 + M_5 + M_6,\end{aligned}$$

where M_j, $j = 1, \dots, 6$, can be estimated by using Lemma 3.7 (super-approximation properties), Lemma 4.1 (estimate of e_n) and (4.7), i.e.,

$$\begin{aligned}|M_1| &\lesssim \|e_\kappa n_h^*\|_{L^2(\Gamma_h^0)} h \|e_\kappa\|_{L^2(\Gamma_h^0)} \lesssim h\|e_\kappa\|^2_{L^2(\Gamma_h^0)}, \\ |M_2| &\lesssim \|e_n\|_{L^2(\Gamma_h^0)}\|e_\kappa n_h^*\|_{L^2(\Gamma_h^0)} \lesssim (h^{-1}\|e_X\|_{L^2(\Gamma_h^0)} + h^k)\|e_\kappa\|_{L^2(\Gamma_h^0)}, \\ |M_3| &\lesssim \|e_n\|_{L^\infty(\Gamma_h^0)}\|e_\kappa\|_{L^2(\Gamma_h^0)}\|e_\kappa n_h^*\|_{L^2(\Gamma_h^0)} \lesssim h\|e_\kappa\|^2_{L^2(\Gamma_h^0)} \quad \text{for} \quad k \geq 4, \\ |M_4| &\lesssim \|d_\kappa\|_{L^2(\Gamma_h^0)}\|e_\kappa\|_{L^2(\Gamma_h^0)}, \\ |M_5| &\lesssim \Big|\int_{\Gamma_h^0} \partial_t e_X \cdot (P_{L^2}(e_\kappa n_h^*) - e_\kappa n_h^*)\Big| + \Big|\int_{\Gamma_h^0} \left(\partial_t(e_X \cdot n_h^*) - (e_X \cdot \partial_t n_h^*)\right) e_\kappa\Big| \\ &\lesssim \left(h\|\partial_t e_X\|_{L^2(\Gamma_h^0)} + \|\partial_t(e_X \cdot n_h^*)\|_{L^2(\Gamma_h^0)} + \|e_X\|_{L^2(\Gamma_h^0)}\right)\|e_\kappa\|_{L^2(\Gamma_h^0)}, \\ |M_6| &\lesssim h^{-2}\|e_X\|_{L^2(\Gamma_h^0)}\|e_\kappa\|_{L^2(\Gamma_h^0)}.\end{aligned}$$

Therefore, combining Lemma 4.2 (a rough estimate of $\partial_t e_X$) and Lemma 4.4 (estimate of $\partial_t[e_X \cdot (n_h^* \circ X_h^*)]$), we can estimate $\|e_\kappa\|_{L^2(\Gamma_h^0)}$ as follows:

$$\begin{aligned}\|e_\kappa\|_{L^2(\Gamma_h^0)} &\lesssim h\|e_\kappa\|_{L^2(\Gamma_h^0)} + h\|\partial_t e_X\|_{L^2(\Gamma_h^0)} + \|\partial_t(e_X \cdot n_h^*)\|_{L^2(\Gamma_h^0)} \\ &\qquad + h^{-2}\|e_X\|_{L^2(\Gamma_h^0)} + \|d_\kappa\|_{L^2(\Gamma_h^0)} + h^k \\ &\lesssim h\|e_\kappa\|_{L^2(\Gamma_h^0)} + h^{-2}\|e_X\|_{L^2(\Gamma_h^0)} + \|d_\kappa\|_{L^2(\Gamma_h^0)} + \|d_v\|_{L^2(\Gamma_h^0)} + h^k.\end{aligned}$$

For sufficiently small h (smaller than some constant), the term $h\|e_\kappa\|_{L^2(\Gamma_h^0)}$ can be absorbed by the left-hand side of the inequality. This yields the result of Lemma 4.5. □

Appendix D. Proof of Lemma 5.1

For the simplicity of notation, we abbreviate $n_h^* \circ X_h^*$ as n_h^* here. The defects $d_v \in S_h(\Gamma_h^0)$ and $d_\kappa \in S_h(\Gamma_h^0)^3$ introduced in (4.1) are characterized by the following relations:

$$\begin{aligned}\int_{\Gamma_h^0} d_v \phi_h &= \Big(\int_{\Gamma_h^0} (v_h^* \cdot n_h^*)\phi_h - \int_{\Gamma^0} (v \cdot n(X))(\phi_h)^l\Big) \\ &\quad - \Big(\int_{\Gamma_h^0} u(X_h^*, t) \cdot n_h^* \phi_h - \int_{\Gamma^0} u(X, t) \cdot n(X)(\phi_h)^l\Big) := G_1 - G_2,\end{aligned} \tag{D.1}$$

and

$$\int_{\Gamma_h^0} d_\kappa \cdot \psi_h = \Big(\int_{\Gamma_h^0} v_h^* \cdot \psi_h - \int_{\Gamma^0} v \cdot (\psi_h)^l\Big) - \Big(\int_{\Gamma_h^0} \kappa_h^* n_h^* \cdot \psi_h - \int_{\Gamma^0} \kappa n(X) \cdot (\psi_h)^l\Big)$$

$$+\Big(\int_{\Gamma_h^0}\nabla_{\Gamma_h^0}X_h^*\cdot\nabla_{\Gamma_h^0}\psi_h-\int_{\Gamma^0}\nabla_{\Gamma^0}X\cdot\nabla_{\Gamma^0}(\psi_h)^l\Big):=G_3-G_4+G_5, \tag{D.2}$$

where $\phi_h\in S_h(\Gamma_h^0)$ and $\psi_h\in S_h(\Gamma_h^0)^3$. Under the conditions of Theorem 2.1, these defects can be estimated by using the following surface perturbation estimates (we refer to [31, Lemma 3.6] and [35, Lemma 5.6] for further details of such results):

$$\Big|\int_{\Gamma_h^0}w\varphi-\int_{\Gamma^0}w^\ell\varphi^\ell\Big|\lesssim h^{k+1}\|w^\ell\|_{L^2(\Gamma^0)}\|\varphi^\ell\|_{L^2(\Gamma^0)} \tag{D.3a}$$

$$\Big|\int_{\Gamma_h^0}\nabla_{\Gamma_h^0}z\cdot\nabla_{\Gamma_h^0}\phi-\int_{\Gamma^0}\nabla_{\Gamma^0}z^\ell\cdot\nabla_{\Gamma^0}\phi^\ell\Big|\lesssim h^{k+1}\|\nabla_{\Gamma^0}z^\ell\|_{L^2(\Gamma^0)}\|\nabla_{\Gamma^0}\phi^\ell\|_{L^2(\Gamma^0)}, \tag{D.3b}$$

where $w,\varphi\in L^2(\Gamma_h^0)$ and $z,\phi\in H^1(\Gamma_h^0)$.

The term G_1 defined in (D.1) can be estimated by using triangle inequality and the surface perturbation estimates in (D.3), i.e.,

$$\begin{aligned}|G_1|\le&\Big|\int_{\Gamma_h^0}(v_h^*\cdot n_h^*)\phi_h-\int_{\Gamma^0}(v_h^*)^l\cdot(n_h^*)^l(\phi_h)^l\Big|\\&+\Big|\int_{\Gamma^0}(v_h^*)^l\cdot(n_h^*)^l(\phi_h)^l-\int_{\Gamma^0}(v\cdot n(X))(\phi_h)^l\Big|\lesssim h^{k+1}\|\phi_h\|_{L^2(\Gamma_h^0)}.\end{aligned}$$

Since $[u(\cdot,t)\circ X_h^*]^l=u(\cdot,t)\circ(X_h^*)^l$ as functions on Γ^0, it follows that (using the Lipschitz continuity of velocity field u) $\|u(X_h^*,t)^l-u(X,t)\|_{L^2(\Gamma^0)}\lesssim\|(X_h^*)^l-X\|_{L^2(\Gamma^0)}\lesssim h^{k+1}$. Then the term $|G_2|$ in (D.1) can be estimated as follows:

$$\begin{aligned}|G_2|\le&\Big|\int_{\Gamma_h^0}u(X_h^*,t)\cdot n_h^*\phi_h-\int_{\Gamma^0}(u(X_h^*,t))^l\cdot(n_h^*)^l(\phi_h)^l\Big|\\&+\Big|\int_{\Gamma^0}(u(X_h^*,t))^l\cdot(n_h^*)^l(\phi_h)^l-\int_{\Gamma^0}u(X,t)\cdot n(X)(\phi_h)^l\Big|\lesssim h^{k+1}\|\phi_h\|_{L^2(\Gamma_h^0)}.\end{aligned}$$

By taking $\phi_h=d_v$ in (D.1) and the estimates of $|G_1|$ and $|G_2|$, we obtain $\|d_v\|_{L^2(\Gamma_h^0)}\lesssim h^{k+1}$.

The term $|G_3|$ defined in (D.2) can also be estimated by using triangle inequality and the surface perturbation estimates in (D.3), i.e.,

$$|G_3|\le\Big|\int_{\Gamma_h^0}v_h^*\cdot\psi_h-\int_{\Gamma^0}(v_h^*)^l\cdot(\psi_h)^l\Big|+\Big|\int_{\Gamma^0}(v_h^*)^l\cdot(\psi_h)^l-\int_{\Gamma^0}v\cdot(\psi_h)^l\Big|\lesssim h^{k+1}\|\psi_h\|_{L^2(\Gamma_h^0)}.$$

The estimate of $|G_4|$ is also similar, with $|G_4|\lesssim h^{k+1}\|\psi_h\|_{L^2(\Gamma_h^0)}$. Moreover, utilizing the second result of (D.3), we have

$$\begin{aligned}|G_5|\le&\Big|\int_{\Gamma_h^0}\nabla_{\Gamma_h^0}X_h^*\cdot\nabla_{\Gamma_h^0}\psi_h-\int_{\Gamma^0}\nabla_{\Gamma^0}(X_h^*)^l\cdot\nabla_{\Gamma^0}(\psi_h)^l\Big|\\&+\Big|\int_{\Gamma^0}\nabla_{\Gamma^0}(X_h^*)^l\cdot\nabla_{\Gamma^0}(\psi_h)^l-\int_{\Gamma^0}\nabla_{\Gamma^0}X\cdot\nabla_{\Gamma^0}(\psi_h)^l\Big|\\\lesssim&\big(h^{k+1}\|\nabla_{\Gamma^0}(X_h^*)^l\|_{L^2(\Gamma^0)}+h^k\big)\|\nabla_{\Gamma_h^0}\psi_h\|_{L^2(\Gamma_h^0)}.\end{aligned}$$

This proves that

$$\|d_\kappa\|_{H_h^{-1}(\Gamma_h^0)}=\sup_{0\neq\psi_h\in S_h(\Gamma_h^0)^3}\frac{\int_{\Gamma_h^0}d_\kappa\psi_h}{\|\psi_h\|_{H^1(\Gamma_h^0)}}\lesssim h^k.$$

Additionally, using the inverse inequality $\|\nabla_{\Gamma_h^0}\psi_h\|_{L^2(\Gamma_h^0)}\le Ch^{-1}\|\psi_h\|_{L^2(\Gamma_h^0)}$, we have $|G_5|\lesssim h^{k-1}\|\psi_h\|_{L^2(\Gamma_h^0)}$. Then, by taking $\psi_h=d_\kappa$ in (D.2) and the estimates of $|G_3|$, $|G_4|$ and $|G_5|$, we obtain $\|d_\kappa\|_{L^2(\Gamma_h^0)}\lesssim h^{k-1}$. □